50 mM Tris-HCl (pH 7.9), 0.1 mM ammonium acetate, 5 mM $MgCl_2$, 2.5 mM DTT, 250 fmol of uncapped RNA substrate, 50 fmol of each ^{32}P-capped RNA (~800 cpm/fmol), and an appropriate amount of purified vRNPs was incubated for 30 min on ice and then irradiated on ice for 10 min with 254-nm UV light (FUNA-UV-Linker FS-1500 [Funakoshi, Japan]) with 0.2 mg/ml of heparin. The ^{32}P-labeled products were digested with nuclease P_1, analyzed by 6% SDS-PAGE, and detected by autoradiography.

Minireplicon assay. Two plasmid vectors carrying a reporter gene (an artificial influenza virus genome containing the firefly luciferase gene of negative polarity, which is synthesized in cells by the human DNA-dependent RNA polymerase I [Pol I]), were constructed as described previously (35). A fragment containing the luciferase gene sandwiched by 5′- and 3′-terminal sequences of FluA/PA/99 and FluB/SH/02 segment 8 was amplified by PCR with specific primers 5′-GTAGTAGAAACAAGGGTGTTTTTTACTCGAGATCTTACAATTTGGACTTTCCGCCCTT-3′ and 5′-GATCCGTCTCCGGGAGCAAAAGCAGGGTGACAAAGACATAATGCATATGGAAGACGCCAAAAACATAAAGAAAGG-3′ for FluA/PA/99 and 5′-TATTCGTCTCAGGGAGCAGAAGCAGAGGATTTGTTTAGTCACTGGCAAACGGAAAAAAATGGAAGACGCCAAAAACATAAAG-3′ and 5′-ATATCGTCTCGTATTAGTAGTAACAAGAGGATTTTATTTTAAATTTACAATTTGGACTTTCCGCC-3′ for FluB/SH/02, using pGV-B (the promoterless luciferase reporter vector; Toyo Inc.) as a template. The amplified PCR products were digested with BsmBI and cloned into pHH21 containing the promoter region of the human rRNA gene (24, 25), which had been digested with BsmBI. The constructed plasmids were designated pHH-A-vNS-Luc and pHH-B-vNS-Luc, in which the luciferase gene in reverse orientation sandwiched with 23- and 26-nucleotide 5′- and 3′-terminal sequences of the FluA/PA/99 segment 8 or 30 and 44-nucleotide 5′- and 3′-terminal sequences of the FluB/SH/02 segment 8, respectively, is placed under the control of the human Pol I promoter. 293T cells were transfected with plasmids for the expression of the FluA minireplicon (pCAGGS-Panama-PB1, pCAGGS-Panama-PB2-cFLAG, pCAGGS-Panama-PA, pCAGGS-Panama-NP, and pHH-A-vNS-Luc) or FluB minireplicon (pCAGGS-Shanghai-PB1, pCAGGS-Shanghai-PB2-cFLAG, pCAGGS-Shanghai-PA, pCAGGS-Shanghai-NP, and pHH-B-vNS-Luc). A plasmid for the expression of *Renilla* luciferase driven by the simian virus 40 (SV40) promoter was used as an internal control for the dual-luciferase assay. As a negative control, 293T cells were transfected with the same plasmids, except for the omission of the PB2 expression plasmid. After transfection, the cells were incubated at 37°C for 24 h, and then the luciferase activity was determined using commercially available reagents (Promega) according to the manufacturer's protocol. The relative luminescence intensity was measured with a luminometer for 20 s. To measure the levels of accumulation of viral mRNA, cRNA, and vRNA, quantitative RT-PCR was performed. Total RNA was extracted from transfected cells and then reverse transcribed with either (i) oligo$(dT)_{20}$ for synthesizing cDNA from viral mRNA, (ii) 5′-ATATCGTCTCGTATTAGTAGTAACAAGAGCATT-3′, which is complementary to the 3′ portion of cRNA of the reporter gene, for synthesizing cDNA from cRNA, or (iii) 5′-TCCATCACGGTTTTGGAATGTTTACTACAC-3′, which is complementary to vRNA, for synthesizing cDNA from vRNA of the reporter gene. These single-stranded cDNAs were subjected to real-time quantitative PCR analyses (Thermal Cycler Dice real-time system TP800; TaKaRa) with SYBR Premix Ex *Taq* (TaKaRa) and two specific primers, 5′-TCCATCACGGTTTTGGAATGTTTACTACAC-3′, corresponding to the firefly luciferase mRNA between nucleotide sequence positions 728 and 757, and 5′-GTGCGCCCCCAGAAGCAATTTC-3′, which is complementary to the firefly luciferase mRNA between nucleotide sequence positions 931 and 952. *Renilla* luciferase mRNA was also amplified with two specific primers, 5′-GCAGCATATCTTGAACCATTC-3′, corresponding to the *Renilla* luciferase mRNA between nucleotide sequence positions 598 and 618, and 5′-CATCACTTGCACGTAGATAAG-3′, which is complementary to the *Renilla* luciferase mRNA between nucleotide sequence positions 725 and 745. The relative amounts of mRNA, cRNA, and vRNA were calculated by using the second-derivative maximum method and normalized to the amount of *Renilla* luciferase mRNA. The ratio of the amounts of mRNA and cRNA relative to vRNA is shown.

Detection of capped RNA copurified with the viral RNA polymerase. 293T cells were transfected with plasmids for the expression of the FluB viral proteins, PB1, FLAG-tagged PB2 (wild-type or mutated PB2), and PA. At 24 h posttransfection, cells were resuspended in a lysis buffer (20 mM Tris-HCl [pH 7.9], 100 mM NaCl, 30 mM KCl, and 0.1% Nonidet P-40). The RNA polymerase complex composed of PB1, FLAG-tagged PB2, and PA was purified by incubation with anti-FLAG M2 agarose (Sigma) at 4°C for 3 h and eluted with an elution buffer (50 mM Tris-HCl [pH 7.9], 100 mM ammonium acetate, 5 mM $MgCl_2$, and 10% [vol/vol] glycerol) containing 0.1 mg/ml FLAG peptide (Sigma). RNAs which interact with the viral RNA polymerase was extracted from recombinant RNA polymerase complexes (100 ng of PB1 equivalents) with phenol-chloroform and ethanol precipitated with 20 μg of carrier tRNA. After treatment with calf intestinal alkaline phosphatase (CIAP), which removes free phosphate groups, periodate oxidation under mild conditions followed by β-elimination with aniline was carried out to remove 5′-terminal m^7G from capped RNA, generating RNA with 5′-triphosphate, which is the substrate for vaccinia virus capping enzyme, as described previously (4, 11). The RNA was then recapped using vaccinia virus capping enzyme with [α-^{32}P]GTP as described in the previous section. To measure the amount of ^{32}P-labeled capped RNA, the RNA was digested with tobacco acid pyrophosphatase (TAP) (Sigma) at 37°C for 1 h in a buffer containing 50 mM sodium acetate (pH 5.5), 5 mM EDTA, and 10 mM 2-mercaptoethanol. The reaction product was analyzed by thin-layer chromatography on a PEI-cellulose plate as described above, and the amount of [^{32}P]m^7Gp was measured with a liquid scintillation counter.

RESULTS

***In vitro* capped RNA cleavage reaction and subsequent RNA elongation reaction.** The FluA polymerase requires the cap1 structure ($m^7GpppNm$) stringently for transcription (4). In contrast, little is known about the requirement for the cap structure of the FluB polymerase. Thus, we first examined the efficiency of the capped RNA cleavage reaction and subsequent RNA elongation reaction by FluA and FluB polymerases using cap1-RNA ($m^7GpppGm$-RNA). The cap1-RNA labeled with ^{32}P in the cap structure was incubated with purified vRNP (see Fig. S1A in the supplemental material) in the absence or presence of nucleoside triphosphates (NTPs) (Fig. 1A). RNA products were analyzed by 15% PAGE containing 8 M urea. FluA and FluB polymerases cleaved the cap1-RNA and produced 11- to 13-nucleotide and 11- to 12-nucleotide RNAs, respectively, in the absence of NTPs (Fig. 1A, lanes 2 to 7), indicating that the endonuclease activity of FluB is different from that of FluA in the distance of cleavage site from the cap structure. This cleavage pattern was observed commonly among FluA strains and among FluB strains (see Fig. S1B, lanes 2 to 6, in the supplemental material). The cleaved RNA products were elongated in the presence of NTPs in a dose-dependent manner (Fig. 1A, lanes 8 to 13), but the elongation efficiency of the FluB polymerase was lower than that of the FluA polymerase. We also confirmed that these elongated products contain full-length transcripts from 8 segments and are partially polyadenylated (see Fig. S2 in the supplemental material). To investigate the cap-binding activity of the polymerases, UV cross-linking assays were carried out (Fig. 1B). Cap1-RNA specifically bound to PB2 in both the FluA and FluB polymerases, although the cap-binding activity of FluB PB2 is less (~25%) than that of FluA PB2. These results suggest that the FluA and FluB polymerases are different in their binding to RNA containing the cap1 structure and in their cleavage modes.

Specificity of recognition of cap structures by Flu polymerases. To investigate the specificity of recognition of cap structures by FluA and FluB polymerases, we carried out similar experiments using RNA primers containing various cap structures. To this end, we prepared ^{32}P-labeled RNAs containing differently methylated cap structures, such as $m^7GpppGm$, m^7GpppG, and GpppG, as described in Materials and Methods. After preparation, we analyzed the terminal cap structure using nuclease-digested samples (see Materials and Methods) and thin-layer chromatography on a PEI-cellulose plate. As shown in Fig. 2A, we confirmed that each RNA

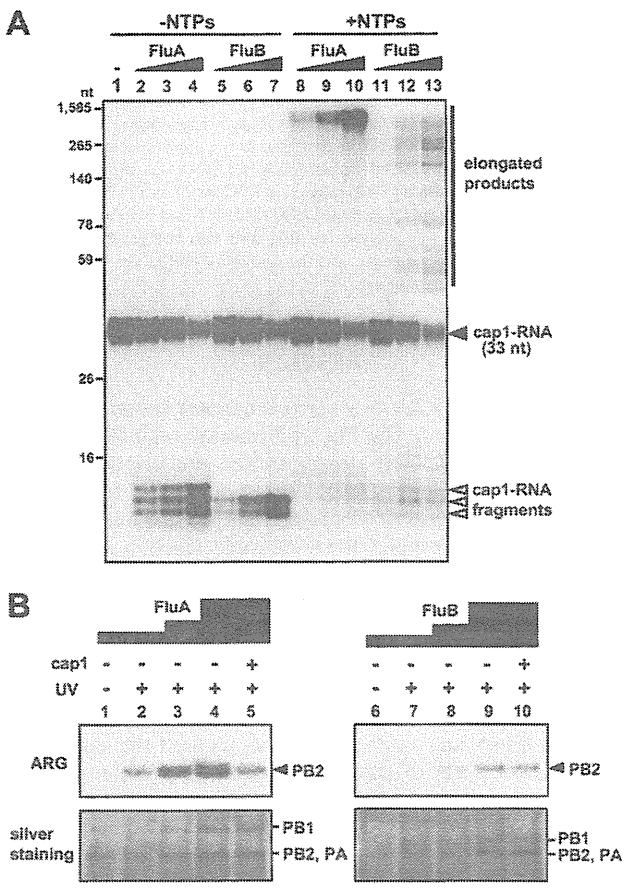

FIG. 1. *In vitro* capped RNA cleavage, RNA elongation and cap-binding reactions. (A) Dose dependency of *in vitro* capped RNA cleavage and subsequent RNA elongation by vRNP. *In vitro* capped RNA cleavage and RNA elongation reactions were performed with 20, 40, and 80 ng of FluA (lanes 2 to 4 and 8 to 10) and FluB (lanes 5 to 7 and 11 to 13) vRNP using 2 fmol of m^7GpppGm-RNA. Capped RNA cleavage was performed in the absence of NTPs (lanes 2 to 7), while RNA elongation was performed in the presence of NTPs (lanes 8 to 13). Synthesized RNA products were analyzed by 15% PAGE containing 8 M urea. (B) Interaction of vRNP with the cap1 structure. UV cross-linking was performed using 50, 100, and 200 ng of FluA (lanes 1 to 5) and FluB (lanes 6 to 10) vRNPs with (lanes 2 to 5 and 7 to 10) or without (lanes 1 and 6) UV irradiation at 254 nm. Competition experiments were performed in the presence of 100 pmol of m^7GpppGm analogue (lanes 5 and 10). Upper panels show autoradiography (ARG), while lower panels show silver staining patterns.

had the expected cap structure. Using these RNAs as substrates, we carried out *in vitro* capped RNA cleavage and subsequent RNA elongation reactions with FluA or FluB vRNPs. As expected, FluA vRNP specifically cleaved both m^7GpppGm-RNA and m^7GpppG-RNA, although the latter was less efficiently cleaved (Fig. 2B, lanes 2, 5, and 8, and D). The m^7GpppGm-RNA fragments were most successfully elongated into viral mRNAs (Fig. 2C, lane 2, and E). In contrast, FluB vRNP could cleave GpppG-RNA efficiently in addition to the m^7GpppGm-RNA and m^7GpppG-RNA (Fig. 2B, lanes 3, 6, and 9, and D). It is noteworthy that m^7GpppGm-RNA fragments also served as an efficient primer for chain elongation, as is the case for the FluA polymerase (Fig. 2C, lane 3, and E). Moreover, we carried out UV cross-linking assays using RNA primers containing various cap structures (Fig. 2F). Interestingly, the cap-binding activity was detected just using m^7GpppGm-RNA with both FluA and FluB vRNPs. These results indicate that the guanine-7-methyl residue is a key for stable cap binding of both FluA and FluB polymerases. It is also indicated that the cap-binding activity is strictly related to the elongation efficiency but not to the cleavage reaction. It is presently unknown why the binding of GpppG and m^7GpppG was not detected under the conditions employed, while m^7GpppG-RNA was recognized and cleaved by both FluA and FluB polymerases and GpppG-RNA was by the FluB polymerase. Since m^7GpppG-RNA and GpppG-RNA were not effective for elongation, the cleavage of these cap structures would be abortive for transcription, possibly due to improper recognition.

Identification of key amino acids involved in the cap recognition specificity of the PB2 subunit of the FluB polymerase. To clarify the cap recognition mechanism, we focused our structure-related functional studies on the interaction between the cap1 structure and the PB2 subunit, which has the cap-binding domain. It is quite likely that amino acid residues essential for cap binding are conserved between FluA and FluB (Fig. 3A). Three-dimensional (3D) structural studies (12) revealed that in the FluA PB2 cap-binding domain (Fig. 3B), Phe404 and His357 sandwich the methylated guanine and Phe323 stacks on the ribose of m^7GTP. Glu361 makes hydrogen bonds with the N1 and N2 positions of guanine, and Lys376 also makes a hydrogen bond with position O6 of guanine. Computer-associated modeling could make the FluB PB2 cap-binding domain fit on the FluA PB2 cap-binding domain (Fig. 3C). In the model of the FluB cap-binding domain, 2 amino acids, Gln325 and Trp359, are different from Phe323 and His357 of the FluA cap-binding domain, respectively.

To determine key amino acids related to the cap recognition specificity, the transcription activity was measured using a minireplicon assay system. In this assay system, we have used a transient-transfection system with a viral genome, in which the coding region for a viral gene is replaced with a luciferase reporter gene while *cis*-acting regulatory regions (24) remain intact (35). The cellular RNA polymerase I produces a negative-sense luciferase RNA sandwiched with viral terminal sequences. Luciferase mRNA is synthesized by transcription of the negative-sense RNA with the viral RNA polymerase and NP and subjected to translation. This system has been used to measure the transcription activity of the Flu polymerase (20, 22).

In the case of FluA PB2, His357, with which methylated guanine is stacked, could be replaced by other aromatic residues such as Trp and Phe, while Phe404, which is also involved in stacking methylated guanine, could not be (Fig. 4A). Leu could not substitute for either His357 and Phe404. On the other hand, in the case of FluB PB2, Trp359 could be replaced with other aromatic residues (but with less efficiency than for the FluA polymerase), but Phe406 could be replaced with hydrophobic residues such as Tyr and Leu (Fig. 4B). To confirm the importance of the hydrogen bonds with methylated guanine, Glu361 and Lys376 in FluA PB2 and Glu363 and Lys378 in FluB PB2 were replaced with alanine (Ala). Ala substitutions in FluA PB2 abolished the transcription activity,

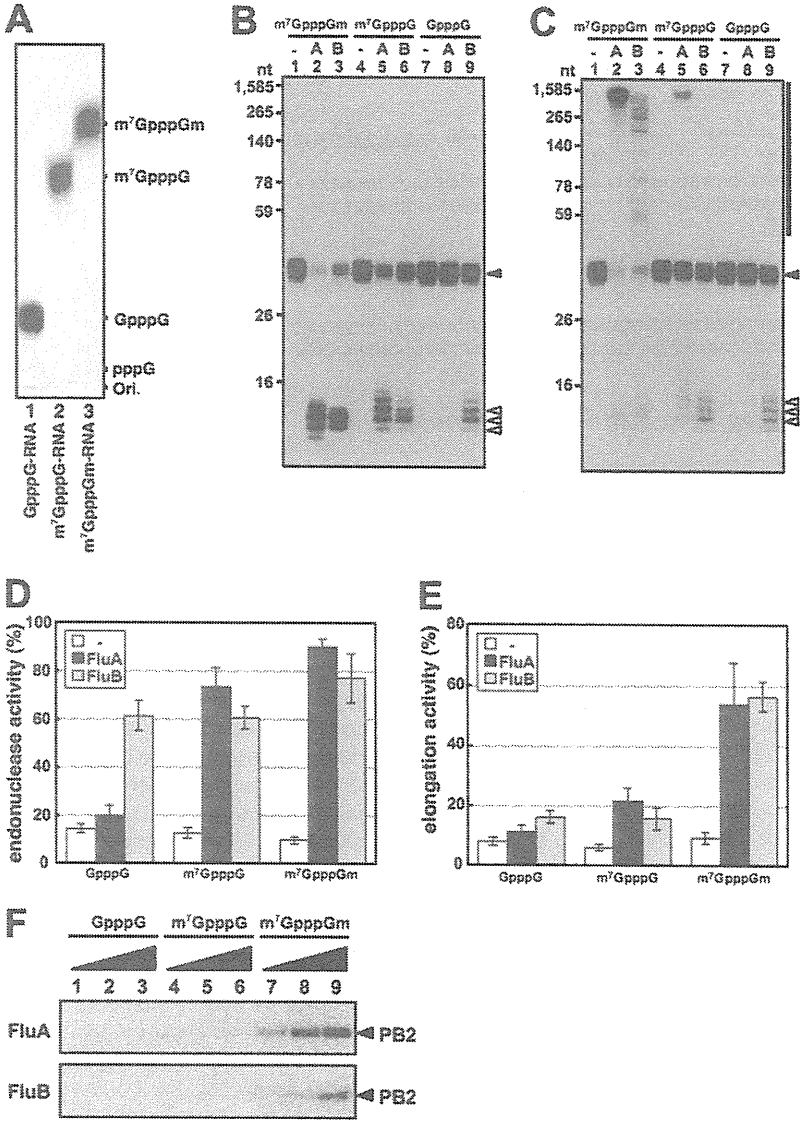

FIG. 2. Specificity of recognition of cap structures by Flu polymerases. (A) Analysis of 5′-terminal cap structures of RNAs. T7 RNA polymerase-synthesized RNAs were treated with nuclease P_1 and analyzed by TLC (PEI-CEL, 0.65 M LiCl), and radioactive nucleotides were detected by autoradiography. (B and C) *In vitro* capped RNA cleavage (B) and RNA elongation (C) reactions were performed with 600 ng of FluA (lanes 2, 5, and 8) or FluB (lanes 3, 6, and 9) vRNP using 2 fmol of variously methylated capped RNAs (m^7GpppGm-RNA, lanes 1 to 3; m^7GpppG-RNA, lanes 4 to 6; GpppG-RNA, lanes 7 to 9). RNA products were analyzed by 15% PAGE containing 8 M urea. The input capped RNAs (33 nt), the cleaved capped RNA products, and the elongated products are indicated as a closed triangle, open triangles, and a black bar, respectively, at the right. (D and E) Ratios of cleaved RNA products (D) and RNA transcripts (E) to total input primer RNAs. (F) Cap-binding activity for variously methylated capped RNAs. UV cross-linking was performed using 50, 100, and 200 ng of FluA (upper panel) and FluB (lower panel) vRNP and 50 fmol of variously methylated capped RNAs (GpppG-RNA, lanes 1 to 3; m^7GpppG-RNA, lanes 4 to 6; m^7GpppGm-RNA, lanes 7 to 9).

while Ala substitution for Lys378 of FluB PB2 caused only a small decrease in the transcription activity (Fig. 4C and D). These results suggest that the stacking interaction of His357 and Phe404 and the hydrogen bonds of Glu361 and Lys376 with methylated guanine are essential for cap recognition by the FluA polymerase. This is in good agreement with a previous report (12). In contrast, it is suggested that the stacking interaction of Trp359 and the hydrogen bonds of Glu363 with methylated guanine are sufficient for cap recognition by the FluB polymerase. These results indicate that the mechanism for recognition of methylated guanine by the FluB polymerase could be different from that for the FluA polymerase. It is also speculated that the cap-binding pocket of the FluB polymerase may be more flexible or less stringent than that of the FluA polymerase in recognition of various cap structures, since Phe406 of FluB PB2 is changeable with other amino acids.

Phe323 in FluA PB2 stacks on the ribose of m^7GTP and was essential for cap recognition (see Fig. S3 in the supplemental

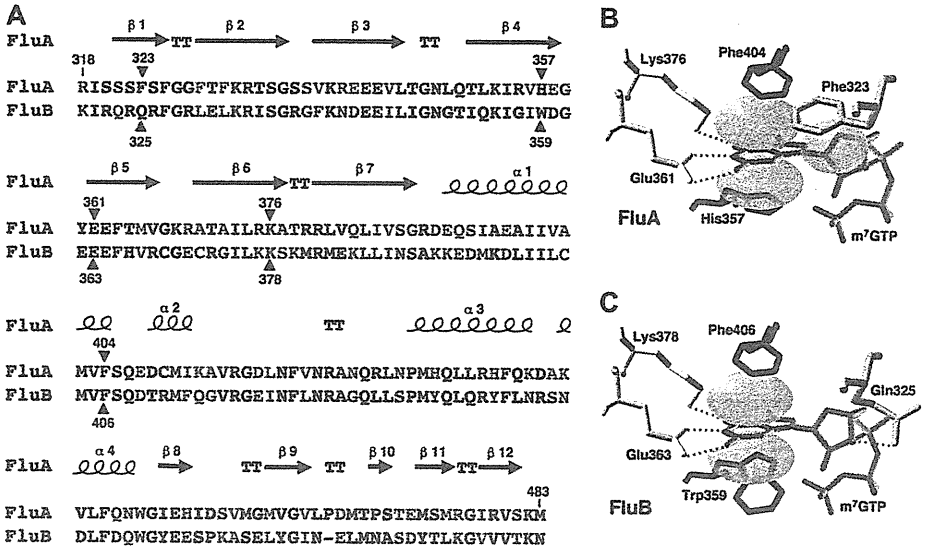

FIG. 3. Structure of the PB2 cap-binding domain. (A) Sequence alignment of the PB2 cap-binding domains of FluA (A/Panama/2007/99) and FluB (B/Shanghai/361/2002). The secondary structure of FluA is displayed over the sequence alignment. Blue letters and green letters show identical residues and similar residues, respectively. Purple triangles indicate the residues in contact with the cap analogue m^7GTP. (B and C) Model of m^7GTP interaction with the cap-binding domains of FluA PB2 (B) (10) and FluB PB2 (C) drawn by computer-associated calculation, with putative hydrogen bonds shown as green dotted lines.

material) (12). However, it is likely that Gln325 in FluB PB2, which is located in the same position of Phe323 in FluA PB2, makes a hydrogen bond with the ribose of m^7GTP. We speculated that FluB PB2 recognizes the cap structure in a flexible pocket as discussed above, so that the hydrogen bonds made by Gln325 and Glu363 could be more crucial for cap binding than those in FluA PB2. In addition, there could be an appropriate amino acid in the amino acid combination between amino acid positions 325 and 363 in FluB PB2 in order to keep the flexible pocket. To confirm this prediction, the transcription activities of mutants with substitutions at position 325 were examined in the presence of the Asp363 mutant (Fig. 4E). The transcription activity of the Asp363 single mutant was reduced to 20% of the wild-type level, possibly because of a longer distance between Asp363 and guanine residues for hydrogen bonds (Fig. 4E; see Fig. S4B in the supplemental material). Interestingly, Lys and Arg mutations but not Ala and Asn mutations at position 325 could rescue the transcription activity of Asp363 (Fig. 4E). We also examined the effect of an Asp363 single mutation and an Arg325-Asp363 double mutation on the transcription and replication processes and the cap-binding activity (Fig. 5). According to the levels of accumulation of mRNA (Fig. 5A) and cRNA (Fig. 5B), the level of reporter expression (Fig. 4E) is well correlated with the transcription but not the replication activities. To examine the cap-binding activity *in vivo*, capped RNAs that could interact with the viral RNA polymerase were coprecipitated from cells expressing the recombinant RNA polymerase, and the cap structure was detected by recapping of RNA which had been CIAP treated and then decapped (β-eliminated) (Fig. 5C). We could detect the [^{32}P]m^7Gp labeled by [α-^{32}P]GTP and vaccinia virus capping enzyme, depending on TAP digestion. In contrast, uncapped RNA treated with CIAP was poorly labeled by this protocol. These results indicate that this recapping method is suitable for the detection of capped RNA specifically. Using this method, we found that the cap-binding activities of these mutants (Fig. 5D) are well correlated with these transcription activities (Fig. 4E) and the mRNA accumulation levels (Fig. 5A). These results indicate that the Arg at position 325 in FluB PB2 supports cap recognition when Glu363 is replaced with Asp363.

DISCUSSION

Most of our knowledge on the transcription mechanism of the influenza virus genome has been derived from studies on FluA, while little has been demonstrated for FluB. This is also the case for studies on the enzymatic aspects of these viral RNA polymerases. Each of the two methyl groups in the cap1 structure, the 7-methyl residue of the guanine base and the 2′-*O*-methyl residue on the ribose of the penultimate base, strongly influences the transcription activity of the FluA polymerase (4). Recently, the structure of the PB2 cap-binding domain of the FluA polymerase with m^7GTP has been clarified (12). Based on these reports, we tried to identify the specificity of cap recognition and characterize key amino acids for cap recognition of the FluB polymerase.

First, we compared the efficiencies of capped RNA cleavage and subsequent RNA elongation reactions of the FluA polymerase with those of the FluB polymerase using cap1-RNA. As expected, the FluA polymerase exhibited efficient endonuclease activity, elongation activity, and cap-binding affinity. The pattern of cleavage of cap1-RNA by the FluB polymerase was different from that by the FluA polymerase (Fig. 1A; see Fig. S1B in the supplemental material), and the RNA elongation and cap-binding activities of the FluB polymerase were lower than those of the FluA polymerase (Fig. 1A and B). These results indicate that the cap binding and cleavage mechanism

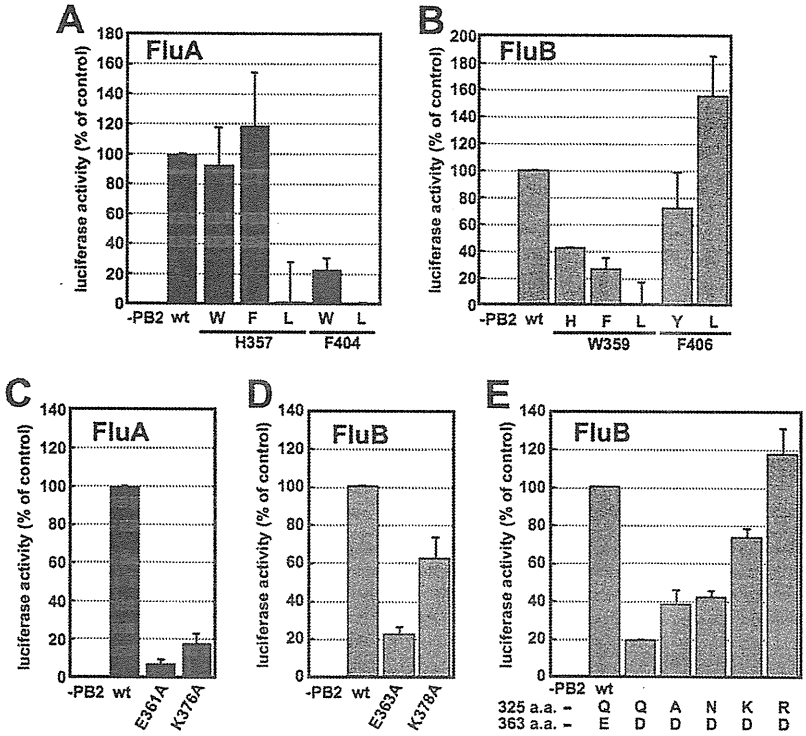

FIG. 4. Transcription activities of PB2 mutants in a minireplicon system. (A and B) Effects of mutations of m^7GTP stacking residues in FluA (A) and FluB (B) PB2 on transcription activity. (C and D) Effects of mutations in residues involved in hydrogen bonds with the guanine residue of m^7GTP in FluA (C) and FluB (D) PB2 on transcription activity. (E) Effect of mutations in Gln325 with an Asp mutation at position 363 in FluB PB2 on transcription activity. The firefly luciferase activity was normalized to *Renilla* luciferase activity. The results are averages and standard deviations (SD) from four independent experiments.

of the FluB polymerase are different from those of the FluA polymerase.

We then examined the specificity of recognition of cap structures by the FluB polymerase compared with that by the FluA polymerase. Using various methylated capped RNAs, we performed capped RNA cleavage and RNA elongation assays (Fig. 2). The FluA polymerase cleaved RNA containing m^7G specifically, while the FluB polymerase could cleave GpppG-RNA as well as RNA containing m^7G. Both the FluA and FluB polymerases elongated and bound to the cap structure efficiently only in the case of $m^7GpppGm$-RNA compared with other capped RNAs (Fig. 2C, 2E, and 2F). Based on these results, we propose that the FluA polymerase recognizes strictly the guanine-7-methyl residue in the cleavage reaction and that the FluB polymerase recognizes only the cap core structure (GpppX), which may result in its weak cap1-binding activity. In addition, these results suggest that the ribose 2′-*O*-methyl residue and/or the guanine-7-methyl residue may be responsible for the elongation reaction by both FluA and FluB polymerases, because cap binding and efficient elongation could not be observed except for $m^7GpppGm$-RNA.

To elucidate the mechanism of cap recognition by the FluB polymerase, we studied the PB2 subunit, which has the cap-binding domain. Recently, the 3D structure of the FluA PB2 cap-binding domain was revealed (12). Amino acid residues essential for cap binding were identified and found to be conserved between FluA and FluB polymerases (Fig. 3A). In the FluA PB2 cap-binding domain (Fig. 3B), the methylated guanine base is sandwiched with His357 and Phe404, and Phe323 stacks on the ribose of m^7GTP. Glu361 makes hydrogen bonds with the N1 and N2 positions of guanine, and Lys376 also makes hydrogen bonds with the O6 position of guanine. Based on the structure of the FluA PB2 cap-binding domain, a model of the FluB PB2 cap-binding domain was postulated (Fig. 3C). Five amino acids which contact the guanine-7-methyl residue are highlighted. Minireplicon assays showed that Trp359 in FluB PB2 is crucial for possible stacking interaction with a methylated guanine base without sandwiching with Phe406 (Fig. 4B). Moreover, the hydrogen bond made by Lys378 to the O6 position of guanine seemed not to be essential for cap recognition (Fig. 4D). These results suggest that the FluB polymerase recognizes the cap structure in a manner different from the FluA polymerase. We illustrated a new proposed computer-associated model for cap recognition by FluB PB2 (see Fig. S4A in the supplemental material), although the 3D structure of the FluB PB2 cap-binding domain has not been determined. The overall structures of four cap-binding proteins, FluA PB2 (12), eIF4E (33, 34), CBP20 (23), and VP39 (16), differ each other widely due to their evolutionarily unrelated origins, but the cap-binding pockets are essentially quite similar (see Fig. S5 in the supplemental material), although there are some differences in details. In addition to the two aromatic amino acids, an acidic residue is directed toward the pocket to accommodate the positively charged π-ring system of

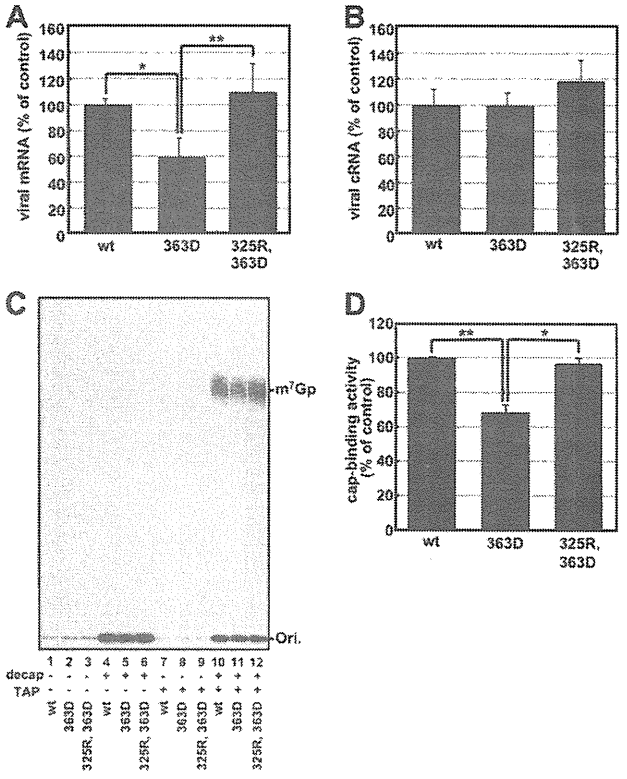

FIG. 5. Suppression mutation in transcription and cap-binding activities for the FluB PB2-363D mutant. (A and B) The levels of accumulation of viral mRNA (A) and cRNA (B) were measured by qPCR. (C) Cap-binding activities of mutants. Coprecipitated capped RNAs with 100 ng of recombinant RNA polymerase complexes (wild type [wt], lanes 1, 4, 7, and 10; 363D mutant, lanes 2, 5, 8, and 11; 325R-363D double mutant, lanes 3, 6, 9, and 12) were recapped before (lanes 1 to 3 and 7 to 9) and after (lanes 4 to 6 and 10 to 12) decapping by β-elimination. Recapped RNAs were treated without (lanes 1 to 6) or with (lanes 7 to 12) tobacco acid pyrophosphatase (TAP) and analyzed by TLC (PEI-CEL, 0.65 M LiCl), and radioactive nucleotides were determined by autoradiography. (D) The radioactivity of [^{32}P]m^{7}Gp of TAP-treated products which were recapped after decapping was counted with a liquid scintillation counter. The cap-binding activity is represented as a ratio to the amount of [^{32}P]m^{7}Gp derived from the wild type. These results are averages and SD from three independent experiments, and the level of significance was determined by Student's *t* test (unpaired) (*, $P < 0.0025$; **, $P < 0.0005$).

the methylated guanine. These amino acids provide high specificity for the recognition of m^{7}GTP and exhibit low affinity for nonmethylated cap analogues (>100-fold difference in affinity compared with N^7-methylated ones) (15, 18, 26). Compared with these well-known cap-binding proteins, the cap-binding pocket of FluB PB2 contains only one aromatic amino acid, Trp359. This feature may cause the low affinity of FluB PB2 for the cap1 structure (Fig. 1B) and the recognition of nonmethylated capped RNA (GpppG-RNA) (Fig. 2) compared with FluA PB2.

In the case of FluA PB2, the stacking interaction of Phe323 with the ribose of m^{7}GTP is also essential for cap recognition. However, Gln325 of FluB PB2 seems to make a hydrogen bond with the ribose of m^{7}GTP instead of a stacking interaction. To examine our speculation that FluB PB2 recognizes the cap structure in the flexible pocket, we made substitution mutations at position 325 in the presence of an Asp363 mutation (Gln → Asp), which should extend too much into the pocket where Gln325 is present. Interestingly, the transcription activity and the cap-binding activity of the Asp363 mutant were restored to the wild-type levels by the Arg325 mutation (Fig. 4E and 5) without changing the replication activity. The transcription activity of the Asp363 single mutant was decreased, possibly because the longer distance between Asp363 and the guanine residue may make hydrogen bonds weak (see Fig. S4B in the supplemental material). These results suggest that the hydrogen bond made by Arg325 with the ribose of the guanosine could support the recognition of the cap structure (Fig. 4E, 5A, 5C, and 5D; see Fig. S4C in the supplemental material). Crystal structure analyses of wild-type FluB PB2 and the mutant containing Arg325 and Asp363 are needed to support our hypothesis.

In summary, our results indicate that the substrate specificity and the residues essential in the cap recognition are different between FluA and FluB polymerases. In the case of the FluA polymerase, m^{7}G-capped RNA is cleaved specifically, and the stacking interactions of His357 and Phe404 with the methylated guanine base and of Phe323 with the ribose of m^{7}GTP and the hydrogen bonds made by Glu361 and Lys376 on the methylated guanine are essential for cap recognition as observed in other cap-binding proteins. In contrast, in the case of the FluB polymerase, unmethylated capped RNA is cleaved as well as m^{7}G-capped RNA, and the stacking interaction which is made only by Trp359 with the guanine base and the hydrogen bonds which are made by Glu363 on the guanine base and by Gln325 with the ribose of m^{7}GTP are enough for cap recognition.

ACKNOWLEDGMENTS

We thank Y. Suzuki and T. Gotanda (Kitasato Institute, Research Center for Biologicals, Saitama, Japan) for providing the purified influenza virus A/Panama/2007/99 and B/Shanghai/361/02 virions. We also thank T. Ogino (Lemer Research Institute, Cleveland Clinic, Cleveland, OH) and A. Kawaguchi (Kitasato Institute for Life Sciences, Kitasato University, Tokyo, Japan) for critical discussion.

This research was supported in part by a grant-in-aid from the Ministry of Education, Culture, Sports, Science, and Technology of Japan (to K.N.).

REFERENCES

1. **Argos, P.** 1988. A sequence motif in many polymerases. Nucleic Acids Res. **16:**9909–9916.
2. **Biswas, S. K., P. L. Boutz, and D. P. Nayak.** 1998. Influenza virus nucleoprotein interacts with influenza virus polymerase proteins. J. Virol. **72:**5493–5501.
3. **Bouloy, M., M. A. Morgan, A. J. Shatkin, and R. M. Krug.** 1979. Cap and internal nucleotides of reovirus mRNA primers are incorporated into influenza viral complementary RNA during transcription in vitro. J. Virol. **32:** 895–904.
4. **Bouloy, M., S. J. Plotch, and R. M. Krug.** 1980. Both the 7-methyl and the 2′-O-methyl groups in the cap of mRNA strongly influence its ability to act as primer for influenza virus RNA transcription. Proc. Natl. Acad. Sci. U. S. A. **77:**3952–3956.
5. **Bouloy, M., S. J. Plotch, and R. M. Krug.** 1978. Globin mRNAs are primers for the transcription of influenza viral RNA in vitro. Proc. Natl. Acad. Sci. U. S. A. **75:**4886–4890.
6. **Braam, J., I. Ulmanen, and R. M. Krug.** 1983. Molecular model of a eucaryotic transcription complex: functions and movements of influenza P proteins during capped RNA-primed transcription. Cell **34:**609–618.
7. **Chen, Z., et al.** 1998. Comparison of the ability of viral protein-expressing plasmid DNAs to protect against influenza. Vaccine **16:**1544–1549.
8. **Dias, A., et al.** 2009. The cap-snatching endonuclease of influenza virus polymerase resides in the PA subunit. Nature **458:**914–918.

9. **Engelhardt, O. G., and E. Fodor.** 2006. Functional association between viral and cellular transcription during influenza virus infection. Rev. Med. Virol. **16:**329–345.
10. **Fodor, E., et al.** 2002. A single amino acid mutation in the PA subunit of the influenza virus RNA polymerase inhibits endonucleolytic cleavage of capped RNAs. J. Virol. **76:**8989–9001.
11. **Fraenkel-Conrat, H., and A. Steinschneider.** 1967. Stepwise degradation of RNA: periodate followed by aniline cleavage. Methods Enzymol. **12B:**243–246.
12. **Guilligay, D., et al.** 2008. The structural basis for cap binding by influenza virus polymerase subunit PB2. Nat. Struct. Mol. Biol. **15:**500–506.
13. **Hara, K., F. I. Schmidt, M. Crow, and G. G. Brownlee.** 2006. Amino acid residues in the N-terminal region of the PA subunit of influenza A virus RNA polymerase play a critical role in protein stability, endonuclease activity, cap binding, and virion RNA promoter binding. J. Virol. **80:**7789–7798.
14. **He, X., et al.** 2008. Crystal structure of the polymerase PA(C)-PB1(N) complex from an avian influenza H5N1 virus. Nature **454:**1123–1126.
15. **Hodel, A. E., P. D. Gershon, X. Shi, S. M. Wang, and F. A. Quiocho.** 1997. Specific protein recognition of an mRNA cap through its alkylated base. Nat. Struct. Biol. **4:**350–354.
16. **Hu, G., P. D. Gershon, A. E. Hodel, and F. A. Quiocho.** 1999. mRNA cap recognition: dominant role of enhanced stacking interactions between methylated bases and protein aromatic side chains. Proc. Natl. Acad. Sci. U. S. A. **96:**7149–7154.
17. **Iwatsuki-Horimoto, K., et al.** 2008. Limited compatibility between the RNA polymerase components of influenza virus type A and B. Virus Res. **135:**161–165.
18. **Izaurralde, E., J. Stepinski, E. Darzynkiewicz, and I. W. Mattaj.** 1992. A cap binding protein that may mediate nuclear export of RNA polymerase II-transcribed RNAs. J. Cell Biol. **118:**1287–1295.
19. **Kawaguchi, A., T. Naito, and K. Nagata.** 2005. Involvement of influenza virus PA subunit in assembly of functional RNA polymerase complexes. J. Virol. **79:**732–744.
20. **Labadie, K., E. Dos Santos Afonso, M. A. Rameix-Welti, S. van der Werf, and N. Naffakh.** 2007. Host-range determinants on the PB2 protein of influenza A viruses control the interaction between the viral polymerase and nucleoprotein in human cells. Virology **362:**271–282.
21. **Lamb, R. A., and P. W. Choppin.** 1977. Synthesis of influenza virus polypeptides in cells resistant to alpha-amanitin: evidence for the involvement of cellular RNA polymerase II in virus replication. J. Virol. **23:**816–819.
22. **Li, C., M. Hatta, S. Watanabe, G. Neumann, and Y. Kawaoka.** 2008. Compatibility among polymerase subunit proteins is a restricting factor in reassortment between equine H7N7 and human H3N2 influenza viruses. J. Virol. **82:**11880–11888.
23. **Mazza, C., A. Segref, I. W. Mattaj, and S. Cusack.** 2002. Large-scale induced fit recognition of an m(7)GpppG cap analogue by the human nuclear cap-binding complex. EMBO J. **21:**5548–5557.
24. **Neumann, G., et al.** 1999. Generation of influenza A viruses entirely from cloned cDNAs. Proc. Natl. Acad. Sci. U. S. A. **96:**9345–9350.
25. **Neumann, G., A. Zobel, and G. Hobom.** 1994. RNA polymerase I-mediated expression of influenza viral RNA molecules. Virology **202:**477–479.
26. **Niedzwiecka, A., et al.** 2002. Biophysical studies of eIF4E cap-binding protein: recognition of mRNA 5′ cap structure and synthetic fragments of eIF4G and 4E-BP1 proteins. J. Mol. Biol. **319:**615–635.
27. **Obayashi, E., et al.** 2008. The structural basis for an essential subunit interaction in influenza virus RNA polymerase. Nature **454:**1127–1131.
28. **Ogino, T., M. Kobayashi, M. Iwama, and K. Mizumoto.** 2005. Sendai virus RNA-dependent RNA polymerase L protein catalyzes cap methylation of virus-specific mRNA. J. Biol. Chem. **280:**4429–4435.
29. **Plotch, S. J., J. Tomasz, and R. M. Krug.** 1978. Absence of detectable capping and methylating enzymes in influenza virions. J. Virol. **28:**75–83.
30. **Shimizu, K., H. Handa, S. Nakada, and K. Nagata.** 1994. Regulation of influenza virus RNA polymerase activity by cellular and viral factors. Nucleic Acids Res. **22:**5047–5053.
31. **Sugiyama, K., et al.** 2009. Structural insight into the essential PB1-PB2 subunit contact of the influenza virus RNA polymerase. EMBO J. **28:**1803–1811.
32. **Tomassini, J. E.** 1996. Expression, purification, and characterization of orthomyxovirus: influenza transcriptase. Methods Enzymol. **275:**90–99.
33. **Tomoo, K., et al.** 2002. Crystal structures of 7-methylguanosine 5′-triphosphate (m(7)GTP)- and P(1)-7-methylguanosine-P(3)-adenosine-5′,5′-triphosphate (m(7)GpppA)-bound human full-length eukaryotic initiation factor 4E: biological importance of the C-terminal flexible region. Biochem. J. **362:**539–544.
34. **Tomoo, K., et al.** 2003. Structural features of human initiation factor 4E, studied by X-ray crystal analyses and molecular dynamics simulations. J. Mol. Biol. **328:**365–383.
35. **Turan, K., et al.** 2004. Nuclear MxA proteins form a complex with influenza virus NP and inhibit the transcription of the engineered influenza virus genome. Nucleic Acids Res. **32:**643–652.
36. **Yuan, P., et al.** 2009. Crystal structure of an avian influenza polymerase PA(N) reveals an endonuclease active site. Nature **458:**909–913.

JOURNAL OF VIROLOGY, July 2011, p. 6197–6204 Vol. 85, No. 13
0022-538X/11/$12.00 doi:10.1128/JVI.00277-11

Replication-Coupled and Host Factor-Mediated Encapsidation of the Influenza Virus Genome by Viral Nucleoprotein▽

Atsushi Kawaguchi,[1,2] Fumitaka Momose,[2] and Kyosuke Nagata[1]*

Department of Infection Biology, Graduate School of Comprehensive Human Sciences, University of Tsukuba, 1-1-1 Tennodai, Tsukuba 305-8575, Japan,[1] and Kitasato Institute for Life Sciences, Kitasato University, 5-9-1 Shirokane, Minato-ku, Tokyo 108-8641, Japan[2]

Received 7 February 2011/Accepted 11 April 2011

The influenza virus RNA-dependent RNA polymerase is capable of initiating replication but mainly catalyzes abortive RNA synthesis in the absence of viral and host regulatory factors. Previously, we reported that IREF-1/minichromosome maintenance (MCM) complex stimulates a *de novo* initiated replication reaction by stabilizing an initiated replication complex through scaffolding between the viral polymerase and nascent cRNA to which MCM binds. In addition, several lines of genetic and biochemical evidence suggest that viral nucleoprotein (NP) is involved in successful replication. Here, using cell-free systems, we have shown the precise stimulatory mechanism of virus genome replication by NP. Stepwise cell-free replication reactions revealed that exogenously added NP free of RNA activates the viral polymerase during promoter escape while it is incapable of encapsidating the nascent cRNA. However, we found that a previously identified cellular protein, RAF-2p48/NPI-5/UAP56, facilitates replication reaction-coupled encapsidation as an NP molecular chaperone. These findings demonstrate that replication of the virus genome is followed by its encapsidation by NP in collaboration with its chaperone.

The genome of influenza type A viruses consists of eight-segmented and single-stranded RNAs of negative polarity. Transcription from the viral RNA (vRNA) genome is initiated using the oligonucleotide containing the cap-1 structure from cellular pre-mRNAs as a primer, whereas genome replication is primer independent and generates full-length vRNA through cRNA (full-sized complementary copy of vRNA) (reviewed in reference 17). Generally, each viral DNA or RNA genome is not present as a naked form but as a complex with viral basic proteins. The influenza virus genome exists as a ribonucleoprotein (termed vRNP) complex with nucleoprotein (NP), one of the basic viral proteins, and viral RNA-dependent RNA polymerases consisting of three subunits (PB1, PB2, and PA). NP binds single-stranded RNA without sequence specificity and is required for maintaining the RNA template in an ordered conformation suitable for viral RNA synthesis and packaging into virions (6, 23, 34). In the case of *Mononegavirales*, nonsegmented and negative-stranded RNA viruses, it is proposed that the nucleocapsid (N) protein forms a trimeric complex with the viral RNA polymerase large (L) protein and phosphoprotein (P) to form a replicase complex to produce the progeny viral genome with concomitant encapsidation of nascent RNA by N protein and that encapsidation is mediated by the chaperone activity of P protein (2, 7, 14, 24). In the case of influenza virus, it is also postulated that NP might regulate the viral polymerase function and encapsidate the virus genome through its interaction with PB1 and/or PB2 (1, 23). Genetic analyses suggest that NP participates in the replication process (15). Recently, it was also shown that NP that is saturated with single-stranded DNA (ssDNA), resulting in the lack of RNA binding activity, stimulates virus genome replication from a model template without primer (18). It is possible that NP stimulates virus genome replication through interaction with the viral polymerase in an RNA binding activity-independent manner. Moreover, the *in vitro* cRNA synthesis using infected cell extracts as an enzyme source depends on a supply of NP free of RNA (27). This finding has been interpreted as indicating that NP prevents the premature termination of RNA synthesis, possibly by binding to nascent RNA chains, that is, encapsidating them. Based on these observations, it could be hypothesized that NP facilitates virus genome replication by both RNA binding- and viral polymerase binding-dependent mechanisms. It is proposed that encapsidation is initiated by successive targeting of exogenous NP monomer to a replicating RNA through the interaction between NP and the viral polymerase, which is distinct from the replicative enzyme bound to the 5′ end of nascent RNA (1, 8, 11, 22), and then additional NP molecules are subsequently recruited by the NP-NP oligomerization (3, 23). It is also reported that nascent cRNA is degraded by host cellular nucleases unless it is stabilized by newly synthesized viral RNA polymerases and NP (33). However, the precise molecular mechanisms involved in virus genome replication and encapsidation by NP are yet unclear.

The cRNA synthesis occurs from incoming vRNA in infected cells, but vRNP complexes isolated from virions by themselves hardly synthesize cRNA (9). Thus, it was reasonable to examine whether a host factor(s) and/or a viral factor(s) is required for the replication process. We reconstituted a cell-free virus genome replication system with virion-associated vRNP and nuclear extracts prepared from uninfected HeLa cells (9). Using biochemical fractionation and complementation assays, we identified influenza virus replication factor 1 (IREF-1) that enabled the viral polymerase to synthesize

* Corresponding author. Mailing address: Department of Infection Biology, Graduate School of Comprehensive Human Sciences, University of Tsukuba, 1-1-1 Tennodai, Tsukuba 305-8575, Japan. Phone and fax: 81 29 853 3233. E-mail: knagata@md.tsukuba.ac.jp.
▽ Published ahead of print on 20 April 2011.

full-sized cRNA. Otherwise, the viral RNA polymerase produces mainly abortive short RNA chains in the absence of IREF-1. IREF-1 was found to be identical with a minichromosome maintenance (MCM) heterohexamer complex. IREF-1/MCM stabilizes replicating polymerase complexes by promoting the interaction between the nascent cRNA and the PA subunit.

Here, we examined the molecular function of NP in influenza virus genome replication using a previously established cell-free virus genome replication system and virion-associated vRNP. Exogenously added NP free of RNA stimulated virus genome replication with MCM in an additive manner. Further, we found that NP activates the viral polymerase during its transition from initiation to elongation to synthesize the unprimed full-length cRNA, but NP by itself is incapable of encapsidating the nascent cRNA. However, we found that RAF-2p48/NPI-5/UAP56/BAT1, which was identified as a host factor for activation of viral RNA synthesis (16), is required for the encapsidation of nascent cRNA with exogenously added NP free of RNA and for the stimulation of the elongation process of virus genome replication. We observed that the level of the virus genome replication was decreased in infected cells when the expression of the RAF-2p48/UAP56 gene was knocked down by small interfering RNA (siRNA)-mediated gene silencing. Based on these observations, we propose an NP- and host factor-dependent mechanism of virus genome encapsidation in concert with its replication.

MATERIALS AND METHODS

Biological materials. vRNP was prepared from purified influenza A/Puerto Rico/8/34 virus as previously described (28). For the expression of His-tagged NP (His-NP), we cloned the open reading frame (ORF) corresponding to the NP gene into pET14b. Rabbit polyclonal antibody against NP was generated by immunization of a 2-month-old female rabbit with His-NP protein. HeLa cells were grown in Dulbecco's modified Eagle's medium (DMEM) supplemented with 10% fetal bovine serum.

Preparation of recombinant proteins. His-tagged recombinant proteins were prepared and purified according to the manufacturer's protocol. In addition, to remove the bacterial RNA possibly bound to NP, we treated recombinant proteins with RNase A before purification and washed them with a buffer containing 1 M NaCl. Recombinant RAF-2p48/UAP56 was prepared from glutathione *S*-transferase (GST)-tagged RAF-2p48/UAP56 by PreScission protease (GE Health Care) digestion. Purified proteins were stored in a buffer containing 50 mM HEPES-NaOH (pH 7.9), 300 mM KCl, 20% glycerol, and 1 mM dithiothreitol (DTT) at −80°C until use. Recombinant MCM complex was prepared as previously described (9). These purified recombinant proteins were separated by SDS-PAGE and visualized by staining with Coomassie brilliant blue in Fig. 1A.

Cell-free virus genome replication system. Cell-free virus genome replication was carried out at 30°C for 90 min in a final volume of 25 μl containing 50 mM HEPES-NaOH (pH 7.9), 5 mM $MgCl_2$, 50 mM KCl, 1.5 mM dithiothreitol, 500 μM each ATP, CTP, and UTP, 25 μM GTP, 5 μCi of [α-^{32}P]GTP (3,000 Ci/mmol), 8 U of RNase inhibitor, and vRNP (10 ng of NP equivalents) in the presence or absence of purified proteins. RNA products were purified, subjected to 4% PAGE in the presence of 8 M urea, and visualized by autoradiography. For limited elongation assays, RNA synthesis was performed with vRNP (150 ng of NP equivalents) in the absence of UTP, and RNA products were separated by 15% PAGE containing 8 M urea. To address the encapsidation of nascent cRNA with NP, RNA synthesis was carried out by following the standard protocol described above except that 0.3 μM UTP, 250 μM each ATP, CTP, and GTP, and 10 μCi of [α-^{32}P]UTP (3,000 Ci/mmol) were used in a final volume of 200 μl. The coprecipitated RNA products with NP or MCM were separated through 10% PAGE containing 8 M urea.

Gene silencing mediated by siRNA. An siRNA against the RAF-2p48/UAP56 gene corresponding to its open reading frame (5′-AGUACUACGUGAAACU GAAGGACAA-3′) and control double-stranded RNA (dsRNA) targeting none of the cellular mRNAs were designed and synthesized by iGENE Therapeutics Inc. HeLa cells (1×10^5 cells) were transfected with 40 pmol of siRNA using Lipofectamine 2000 (Invitrogen) according to the manufacturer's protocol. At 48 h posttransfection, the cells were infected with influenza A/PR/8/34 at a multiplicity of infection (MOI) of 10 in the absence or presence of 100 μg/ml of cycloheximide (CHX). The RAF-2p48/UAP56 knockdown cells were also transfected with viral protein expression plasmids encoding PB1, PB2, PA, and NP and pHH21-vNS-Luc reporter plasmid to reconstitute a model viral replicon (19, 30). This reporter plasmid carries the luciferase (Luc) gene in reverse orientation sandwiched between 23-nucleotide (nt)-long 5′-terminal and 26-nucleotide-long 3′-terminal promoter sequences of the influenza virus segment 8, which is placed under the control of the human polymerase I (Pol I) promoter.

Indirect immunofluorescence assay. HeLa cells on coverslips were fixed with 4% paraformaldehyde in phosphate-buffered saline (PBS). The cells were permeabilized in 0.5% Triton X-100 and incubated in PBS containing 1% bovine serum albumin (BSA). The coverslips were incubated with anti-RAF-2p48/UAP56 rabbit polyclonal antibody (16) for 1 h. After a washing step with 0.1% Tween 20 in PBS, coverslips were incubated with Alexa Fluor 568-conjugated anti-rabbit IgG (Invitrogen) for 1 h. Images were acquired under the same exposure time by a fluorescence microscope system (Axiovision; Carl Zeiss).

Primer extension assay. Total RNAs isolated from control and RAF-2p48/UAP56 knockdown cells at 0, 3, 6, and 9 h postinfection (hpi) were subjected to reverse transcription at 42°C for 1 h with primers specific for segment 5 vRNA (5′-GGGAATACAGAGGGAGAA-3′) corresponding to the NP cDNA between nucleotide sequence positions 1336 and 1354, segment 5 m/cRNA (5′-G ATTTCAGTGGCATTCTGGC-3′) complementary to the NP cDNA between nucleotide sequence positions 101 and 120, and 5S rRNA (5′-GGGGTACCTT CGAAAGCCTACAGCACCCGGTA-3′), which were labeled at their 5′ ends with [γ-^{32}P]ATP and T4 polynucleotide kinase (Toyobo). The products purified with phenol-chloroform extraction and ethanol precipitation were separated through 6% polyacrylamide gel containing 7 M urea and visualized by autoradiography.

Real-time quantitative PCR. Total RNAs isolated from control and RAF-2p48/UAP56 knockdown cells at 12 h posttransfection for construction of the model viral replicon were subjected to reverse transcription with primers to determine the level of vRNA (5′-TCCATCACGGTTTTGGAATGTTTACTA CAC-3′, which corresponds to the luciferase coding region between nucleotide sequence positions 728 and 757), cRNA (5′-AGTAGAAACAAGGGTGTTTT TTAGTA-3′, which is complementary to the 3′ portion of the segment 8 cRNA), and viral mRNA [oligo$(dT)_{20}$ for poly(A) tail] synthesized from the reconstituted model viral replicon. The synthesized single-stranded cDNAs were subjected to real-time quantitative PCR analysis (Thermal Cycler Dice Real Time System TP800; TaKaRa) with two specific primers, 5′-TCCATCACGGTTTTGGAAT GTTTACTACAC-3′, which corresponds to the luciferase coding region between nucleotide sequence positions 728 and 757, and 5′-GTGCGCCCCCAGAAGC AATTTC-3′, complementary to the luciferase coding region between nucleotide sequence positions 931 and 952. The amount of NP mRNA transcribed from the expression plasmid, which is transcribed by cellular RNA polymerase II, was detected as an internal control.

RESULTS AND DISCUSSION

Stimulation of *de novo* cRNA synthesis by NP. Exogenously added recombinant NP free of RNA (here, designated exogenous NP) stimulated *de novo* virus genome replication in the absence of MCM and any kind of primer (Fig. 1B, lanes 1 to 5). We confirmed by RNase H digestion analyses with primers corresponding to each segment that RNA products corresponded to those synthesized from each segment (data not shown). Then, we examined whether exogenous NP and MCM coordinately stimulate the virus genome replication reaction. MCM stimulated virus genome replication additively with recombinant NP, suggesting that NP and MCM function through distinct mechanisms (Fig. 1B, lanes 6 to 10 and 16 to 20). The stimulatory activity per molecule of MCM was five times higher than that of NP, as judged by the slopes of the lines in Fig. 1C (Fig. 1D). We observed that authentic NP free of RNA purified from virions by CsCl glycerol density gradient centrifugation (5, 34) stimulates activity equally as well as recombi-

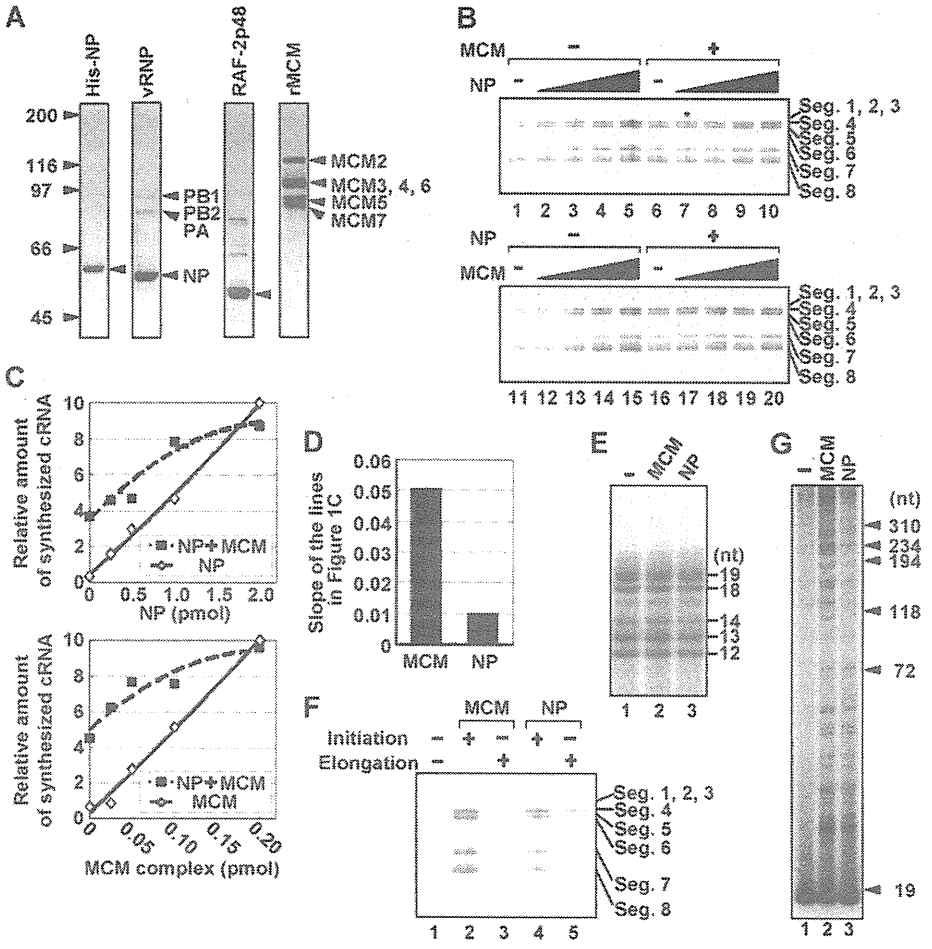

FIG. 1. NP and MCM additively stimulate virus genome replication. (A) Purified recombinant proteins and vRNP. Purified His-NP, vRNP, RAF-2p48/UAP56, and MCM complexes were separated by 7.5% SDS-PAGE and visualized by staining with Coomassie brilliant blue. (B) Stimulatory activity of NP and MCM in cell-free virus genome replication. RNA synthesis was carried out in the absence (lanes 1 to 5) or presence (lanes 6 to 10) of recombinant MCM complex (0.05 pmol of MCM complex) with 0 (lanes 1 and 6), 0.25 (lanes 2 and 7), 0.5 (lanes 3 and 8), 1.0 (lanes 4 and 9), and 2.0 pmol (lanes 5 and 10) of recombinant NP (upper panel). For the experiments shown in the lower panel, we performed the RNA synthesis assay in the absence (lanes 11 to 15) or presence (lanes 16 to 20) of recombinant NP (0.50 pmol) with 0 (lanes 11 and 16), 0.025 (lanes 12 and 17), 0.05 (lanes 13 and 18), 0.10 (lanes 14 and 19), and 0.20 pmol (lanes 15 and 20) of MCM complex (lower panel). (C) Quantitative summary of panel A. The amounts of newly synthesized cRNA corresponding to segment 7 were determined by the ImageJ software. (D) Stimulatory activity per molecule of MCM and NP. The slopes of the lines in the presence of NP or MCM in panel C were determined. (E) Limited elongation assays. Unprimed limited elongation assays were carried out in the absence (lane 1) or presence (lane 2; 0.5 pmol) of MCM or NP (lane 3; 3.0 pmol). (F) NP functions during transition from initiation to elongation reaction. Unprimed limited elongation reactions were performed without (lanes 1, 3, and 5) or with (lanes 2 and 4) either MCM (lane 2; 0.5 pmol) or NP (lane 4; 3.0 pmol). After incubation for 1 h, elongation reactions were restarted by the addition of UTP. For lanes 3 and 5, MCM (0.5 pmol) and NP (3.0 pmol) were added at the restart of elongation reaction, respectively. (G) MCM stimulates the elongation process more effectively than NP. RNA synthesis was carried out in the absence (lane 1) or presence of either MCM (lane 2; 0.5 pmol) or NP (lane 3; 3.0 pmol) with 0.3 μM UTP, 250 μM each ATP, CTP, and GTP, and 10 μCi of [α-^{32}P]UTP (3,000 Ci/mmol). The purified products were separated through 4 to 15% linear gradient PAGE containing 8 M urea and visualized by autoradiography.

nant NP (data not shown). We used as the enzyme source the vRNP containing authentic NP that is bound to the template RNA. Thus, it is quite likely that RNA-free NP but not template-bound NP is required for *de novo* virus genome replication. The RNA synthesis level varied among segments, as previously described (9). For instance, segments 1, 2, and 3 were hardly replicated compared with replication of other segments. The reason for this variation in cRNA synthesis is presently unknown.

NP facilitates the promoter escape of the viral RNA polymerase. Previously, we demonstrated that MCM does not enhance the frequency of replication initiation, but rather makes a nonproductive viral polymerase override the step for abortive synthesis. To examine whether NP is involved in the initiation reaction of virus genome synthesis, we carried out a limited elongation assay, in which UTP is omitted from the reaction mixture and the RNA polymerase pauses at the first adenine residue on the template. The expected lengths of limited elon-

gation products are 12 nt for segments 1, 3, and 7, 13 nt for segments 5 and 8, 14 nt for segment 6, 18 nt for segment 4, and 19 nt for segment 2. Since we detected comparable amounts of each RNA product in the absence or presence of exogenous NP (Fig. 1E), it is concluded that NP, like MCM, does not stimulate the initiation reaction (9). Thus, NP may be required for a step(s) after the initiation and the early elongation steps, in which short cRNAs are synthesized.

To examine whether NP stimulates the transition of the viral polymerase from initiation to elongation, that is, the promoter escape of the viral polymerase, unprimed limited elongation assays were first performed in the absence of UTP, and elongation reactions were restarted by the addition of UTP (Fig. 1F). MCM (0.5 pmol) or exogenous NP (3 pmol) was also added either before or after the limited elongation. The full-length cRNA was synthesized by restarting the limited elongation reaction performed in the presence of MCM (lane 2) or exogenous NP (lane 4) during the limited elongation reaction. Thus, it is quite likely that, to avoid abortive RNA synthesis by the viral polymerase, MCM and NP are required for the viral polymerase prior to its movement along a 12- to 19-nt-long vRNA template from the 3′ terminus of vRNA, where the hairpin loop and double-stranded promoter region are located. Since the initiation reaction was not stimulated by NP (Fig. 1E) and since the viral polymerase could not transit from initiation to elongation in the absence of NP (Fig. 1F), it is possible that NP stimulates elongation complexes during the promoter escape of the viral polymerase, as does MCM (9). A cell-free virus genome replication reaction was also carried out (Fig. 1G) in the presence of MCM (lane 2; 0.5 pmol) or NP (lane 3; 3 pmol) with a low concentration of UTP to slow down the reaction and synthesize a ladder of nascent cRNA chains in order to examine the length of elongated nascent cRNA chains. We found that comparable amounts of cRNA with a shorter length (~100 nt) are synthesized in the presence of either MCM or NP. In contrast, the amount of longer cRNAs (>100 nt) stimulated by MCM was greater than that stimulated by NP (Fig. 1G, compare lane 2 with lane 3). Therefore, it is quite likely that MCM promotes the elongation process more effectively than NP, possibly due to the weak interaction of exogenously added NP with long nascent cRNA, as described later. Taking these results together, it is strongly suggested that NP, like MCM, stimulates the promoter escape of the viral polymerase. Previous reports showed that the target of MCM is PA (9), whereas that of NP is PB1 and PB2 (1). Therefore, it is possible that the replication stimulation mechanisms of NP and MCM are distinct from each other.

Encapsidation of newly synthesized virus genome by NP. Previously, we proposed that MCM stimulates virus genome replication by acting as a scaffold between nascent cRNA chains and the viral polymerase during the promoter escape of the polymerase (9). Since NP has both RNA and viral polymerase binding activities, it should be speculated that NP, like MCM, also functions as a scaffold between newly synthesized RNA and the viral polymerase. To address this, we tried to pull down the replicated cRNA chains associated with His-tagged MCM or NP using Ni-nitrilotriacetic acid (NTA) resin (Fig. 2A). The cell-free virus genome replication reaction was carried out in the presence of an equal molar amount of MCM (lanes 1 and 3) or NP (lanes 2 and 4) with a low concentration

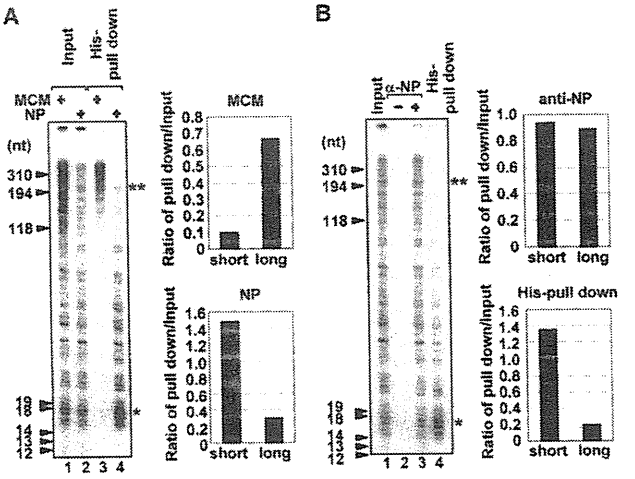

FIG. 2. Encapsidation of nascent cRNA with NP. (A) *De novo* RNA synthesis was carried out in the presence of His-MCM (lanes 1 and 3; 20 pmol) or His-NP (lanes 2 and 4; 20 pmol) with 0.3 μM UTP and 250 μM each ATP, CTP, and GTP and 10 μCi of [α-^{32}P]UTP (3,000 Ci/mmol) in a final volume of 200 μl. The products were purified with His-MCM (lane 3) or His-NP (lane 4) by using Ni-NTA resin. Lanes 1 and 2 represent 20% of the input amounts. The band intensities of short (*) and long (**) nascent cRNA products were quantitatively measured with ImageJ software, and the relative intensity of newly synthesized cRNA coprecipitated with MCM or NP against the input fraction is indicated. (B) *De novo* RNA synthesis was carried out with the authentic vRNP in the presence of His-NP as described for panel A. The newly synthesized RNA products were coimmunoprecipitated without (lane 2) or with (lane 3) anti-NP antibody. Lane 1 shows 20% of the input amount. The product purified by Ni-NTA resin is also represented in lane 4. The band intensities of short (*) and long (**) nascent cRNA products were quantitatively measured with ImageJ software, and the relative intensity of newly synthesized cRNA precipitated by using anti-NP antibody or Ni-NTA resin against input fraction is indicated. α, anti.

of UTP in order to examine the length of copurified RNA as shown in Fig. 1G. As shown in input lanes, MCM stimulated the elongation process more effectively than NP (Fig. 1E and 2A, lanes 1 and 2). Further, longer nascent cRNA chains were preferentially copurified with MCM (Fig. 2A, lane 3), suggesting that MCM stabilizes the elongation complex and thereby makes the viral polymerase escape the promoter successfully. It also seems likely that MCM has a role in the elongation process, but its precise mechanism is still unknown. In contrast, rather shorter cRNA chains were associated with exogenous NP (lane 4). After or along with virus genome replication, the newly synthesized virus genome has to be encapsidated by exogenous NP to form RNP complexes as templates for the next phase of virus genome replication and to protect the virus genome from degradation by cellular nucleases (33). It is hypothesized that encapsidation proceeds by targeting exogenous NP to the nascent RNA through the interaction between NP and the viral polymerase bound to the 5′ end of the nascent RNA to allow NP to interact with the viral RNA preferentially with respect to other cellular RNA species (1, 8, 11, 22), and then subsequently NP is recruited through NP-NP oligomerization (3, 23). In our cell-free system, we found that exogenous NP interacts with shorter cRNA (Fig. 2A, lane 4) without the addition of soluble viral polymerases, which could bind to

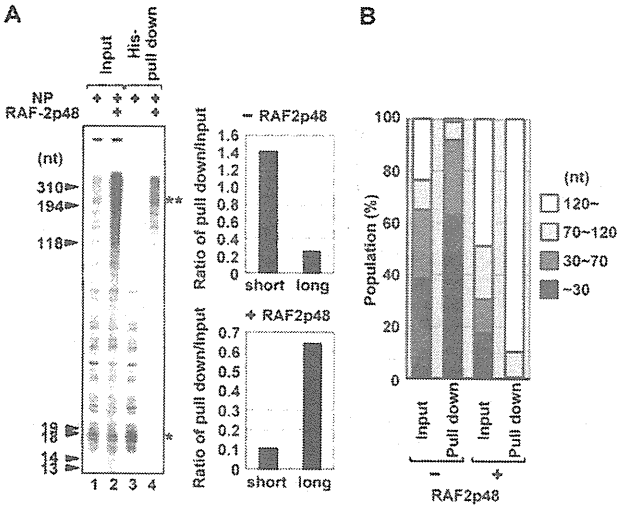

FIG. 3. The stimulatory activity of RAF-2p48/UAP56 in encapsidation of nascent cRNA. (A) RNA synthesis was performed in the absence (lanes 1 and 3) or presence (lanes 2 and 4) of recombinant RAF-2p48/UAP56 with His-NP as described in the legend of Fig. 2. The products were purified with His-NP by using Ni-NTA resin (lanes 3 and 4). Twenty percent of the input amounts is shown in lanes 1 and 2. The band intensities of short (*) and long (**) nascent cRNA products were quantitatively measured with ImageJ software, and the relative intensity of cRNA coprecipitated with NP in the absence or presence of RAF-2p48 against input fraction is indicated. (B) The band intensities of the regions corresponding to RNAs of less than 30 nt, 30 to 70 nt, 70 to 120 nt, and more than 120 nt in each lane in panel A were quantitatively measured with ImageJ software, and the results are indicated as a percentage of the total intensity of each lane.

the 5′ end of the nascent RNA and be a target of NP. It might be explained that the primary targeting of NP to the nascent RNA easily occurs since there is no RNA target other than the nascent RNA in our system. However, it is worth noting that encapsidation of longer nascent cRNA by NP was not achieved when NP was simply added to the system (lane 4). This raises a question of how the newly synthesized virus genome is encapsidated with NP free of RNA.

NP recognizes the phosphodiester backbone of ssRNA in a specific sequence-independent manner. We used, as the enzyme source, the vRNP containing authentic NP, which is bound to the template RNA. Thus, it is reasonably hypothesized that newly synthesized cRNA chains remain associated with the template RNP, possibly by partial hybridization of the nascent cRNA with template vRNA and/or the interaction of nascent cRNA with template-bound authentic NP instead of exogenous NP. To address this, we immunopurified the template-bound authentic NP of vRNP in the presence of exogenous His-NP using anti-NP antibody (Fig. 2B). The length of RNA products associated with authentic NP or both authentic NP and exogenous His-NP (lane 3) was clearly distinct from that of RNA products interacting with only exogenous His-NP (lane 4). From these results, it is assumed that the nascent cRNA product is hardly encapsidated with exogenous NP since the nascent cRNA tends to interact more with template-bound NP than exogenous NP and might partially hybridize with the template.

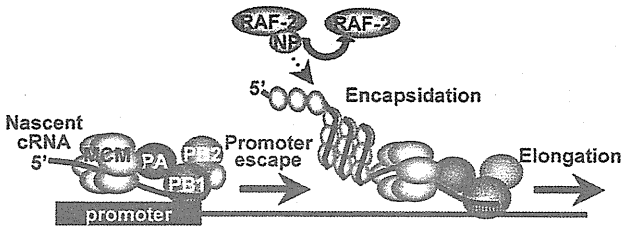

FIG. 4. Proposed model. NP facilitates the promoter escaping from the viral polymerase through the interaction between NP and the viral polymerase in an RNA binding activity-independent manner. During elongation step, RAF-2p48/UAP56 stimulates the coreplicational encapsidation of newly synthesized cRNA with exogenous NP, thereby increasing the processivity of the viral polymerase.

Encapsidation with NP mediated by RAF-2p48/UAP56. As shown in Fig. 2, it is assumed that some factor(s) may be missing in the encapsidation of nascent cRNA products with exogenous NP. Previously, RAF-2p48/UAP56/BAT1 (here, designated RAF-2p48/UAP56) belonging to the DExD-box family of ATP-dependent RNA helicase (13), also reported as NPI-5 (20), was identified as a host factor that binds to NP and stimulates influenza virus RNA synthesis from exogenously added model vRNA templates (16) and that is involved in splicing of cellular pre-mRNAs and messenger RNP maturation of cellular and viral transcripts (4, 25, 29). RAF-2p48/UAP56 binds to NP free of RNA but not to an NP-RNA complex and facilitates NP-RNA complex formation as a molecular chaperone for NP. Therefore, it was proposed that RAF-2p48/UAP56 is involved in the arrangement of NP on the template. However, its precise roles, including the requirement for the encapsidation process, have not yet been uncovered. Thus, we tried to examine whether RAF-2p48/UAP56 facilitates the encapsidation of newly synthesized RNA with exogenous NP (Fig. 3A). We found that long nascent cRNA was encapsidated with exogenous NP by the addition of RAF-2p48/UAP56 (Fig. 3A, compare lane 4, in which RAF-2p48/UAP56 is present, with lane 3, in which RAF-2p48/UAP56 is absent). The ATP-dependent RNA unwinding activity of RAF-2p48/UAP56 was not required for the encapsidation of nascent chains since the encapsidation occurred in the presence of ATPγS, which is a nonhydrolyzable analog of ATP (data not shown). Therefore, we propose a model whereby RAF-2p48/UAP56 facilitates the formation of RNP complexes by coreplicationally transferring exogenous NP to the nascent cRNA chain. It is unlikely that RAF-2p48/UAP56 remodels secondary structures of template and newly synthesized cRNA by its potential RNA helicase activity (Fig. 4). Furthermore, RAF-2p48/UAP56 stimulated the elongation activity of the viral polymerase, possibly by facilitating the encapsidation of nascent cRNA (Fig. 3, lane 2). It is speculated that the coreplicational encapsidation of nascent cRNA by NP may prevent the premature termination of RNA synthesis by avoiding a secondary structure of nascent RNA, which is hypothesized to be one of the causative factors in the termination process of other RNA polymerases (10, 27). Therefore, it is possible that the encapsidation of the nascent RNA with exogenous NP mediated by RAF-2p48/UAP56 increases the processivity of the

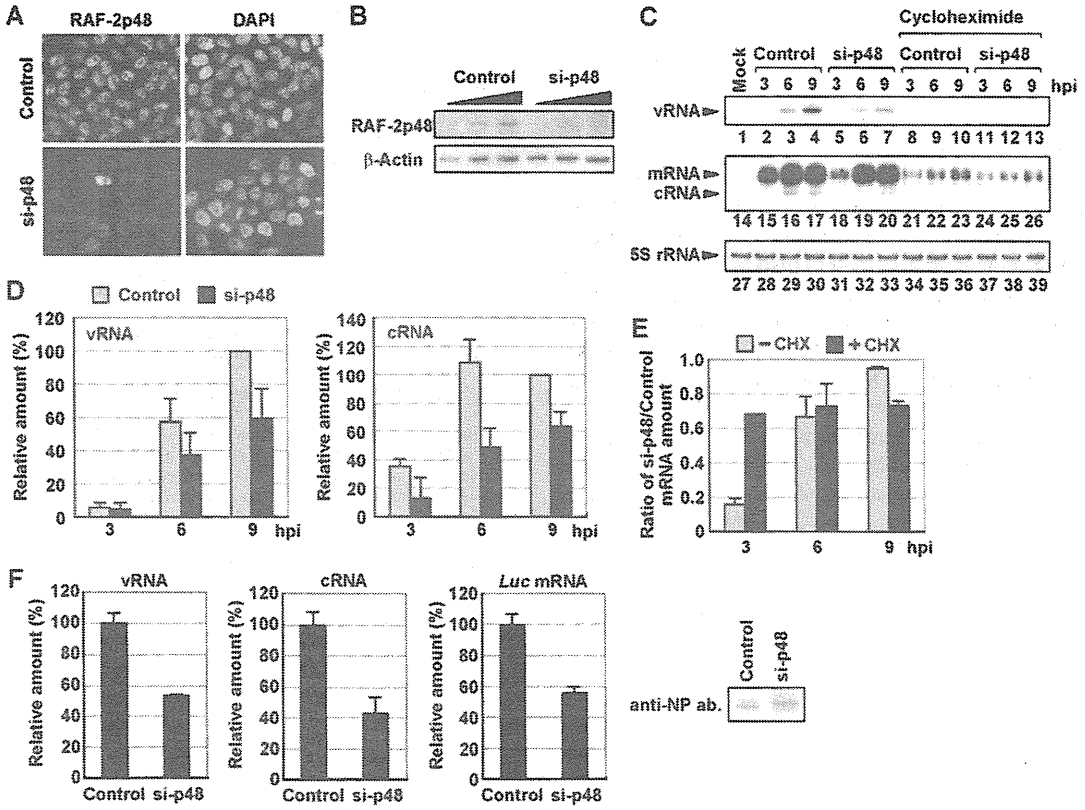

FIG. 5. Involvement of RAF-2p48/UAP56 in influenza virus genome replication in infected cells. (A) At 48 h posttransfection, cells transfected with either a control or siRNA against the RAF-2p48/UAP56 ORF (si-p48) were subjected to indirect immunofluorescence assay with anti-RAF-2p48/UAP56 antibody. Nuclear DNA stained with 4′,6-diamidino-2-phenylindole (DAPI) is also shown. Images were acquired under the same exposure time by a fluorescence microscope system (Axiovision; Carl Zeiss). (B) Expression level of RAF-2p48/UAP56. The lysates prepared from control and RAF-2p48/UAP56 knockdown cells (5×10^3, 1×10^4, and 2×10^4 cells) were separated by SDS-PAGE and then visualized by Western blotting assays with anti-NP and β-actin antibodies. (C, D, and E) Level of viral RNAs in infected RAF-2p48/UAP56 knockdown cells. Control and RAF-2p48/UAP56 knockdown cells were infected with influenza virus in the absence (lanes 1 to 7 and 14 to 20) or presence of cycloheximide (lanes 7 to 13 and 21 to 26) for 0, 3, 6, and 9 h. Primer extension assays were carried out with primers specific for segment 5 vRNA or m/cRNA as described in Materials and Methods. As a loading control, 5S rRNA was also detected (lanes 27 to 39). The band intensities were quantitatively measured by ImageJ software, and the results of three independent experiments are summarized in panel D and are indicated in panel E as the ratio of the mRNA amount in RAF-2p48/UAP56 knockdown cells to that in control cells with or without CHX. (F) The level of viral RNAs synthesized from a reconstituted model replicon in RAF-2p48/UAP56 knockdown cells. Control and RAF-2p48/UAP56 knockdown cells were transfected with plasmids expressing PB1, PB2, PA, and NP and model vRNA encoding the luciferase gene as described in Materials and Methods. At 12 h posttransfection, total RNAs were purified and then subjected to reverse transcription, followed by quantitative real-time PCR with primer sets specific for vRNA, cRNA, and luciferase mRNA. The expression level of NP protein in control and RAF-2p48/UAP56 knockdown cells was also detected by a Western blotting assay with anti-NP antibody (ab).

viral polymerase by avoiding inappropriate secondary structures of nascent cRNA.

Involvement of RAF-2p48/UAP56 in influenza virus genome replication in infected cells. Finally, we tried to examine whether RAF-2p48/UAP56 functions in influenza virus genome replication in cultured cells using siRNA-mediated gene silencing. At 48 h posttransfection of siRNA corresponding to the RAF-2p48/UAP56 ORF, the expression level of RAF-2p48/UAP56 in knockdown cells decreased to approximately 30% of that of cells transfected with the nontargeting siRNA used as a negative control (Fig. 5A and B). We carried out quantitative primer extension assays with appropriate primers specific for each vRNA and mRNA/cRNA of segment 5 (Fig. 5C and D). We confirmed that the product corresponding to cRNA was not found from a fraction bound with oligo(dT) cellulose (data not shown). This result showed that the accumulation of vRNA and cRNA was reduced and delayed in RAF-2p48/UAP56 knockdown cells compared with levels in control cells (Fig. 5C, lanes 1 to 7 and 14 to 20, and D). The same results were obtained for other segments (data not shown). It is proposed that nascent cRNA is degraded unless it is encapsidated with viral RNA polymerase and NP (33). In addition, the results shown in Fig. 3 and a previous report (16) demonstrated that RAF-2p48/UAP56 stimulates the viral polymerase activity. Thus, RAF-2p48/UAP56 might be involved in virus genome replication and encapsidation in infected cells. We also found that the level of NP mRNA in RAF-2p48/UAP56 knockdown cells decreased to 15% in control cells at 3 hpi (Fig. 5C, lanes 15 and 18, and E). In contrast, comparable amounts of NP mRNA were found in both control and RAF-

2p48/UAP56 knockdown cells at 6 and 9 hpi (Fig. 5C, lanes 16, 17, 19, and 20) since the amount of vRNA template sufficient for viral mRNA synthesis might be accumulated at 6 and 9 hpi, but the replication activity was reduced and delayed in RAF-2p48/UAP56 knockdown cells. To confirm the effect of RAF-2p48/UAP56 on viral transcription, we utilized cycloheximide (CHX), a potent protein synthesis inhibitor (Fig. 5C, lanes 8 to 13 and 21 to 26, and E). A previous report showed that CHX suppresses viral protein synthesis and thereby leads to degradation of replicated viral RNA but not mRNA since new vRNP formation was repressed (33). Therefore, we could examine the amount of viral mRNA synthesized from incoming vRNP independent of the level of vRNA accumulation in the presence of CHX (Fig. 5C, lanes 8 to 13, and E). The level of NP mRNA in RAF-2p48/UAP56 knockdown cells was reduced to 70% in control cells in the presence of CHX at 3 hpi (Fig. 5C, lanes 21 and 24, and E). Therefore, it is likely that the reduction of viral mRNA synthesis in RAF-2p48/UAP56 knockdown cells is mainly due to the decrease of vRNP accumulation in the absence of CHX although RAF-2p48/UAP56 has a stimulatory role in viral transcription, possibly by arrangement of NP on template and/or the nuclear export-competent messenger RNP formation (25). To rule out the possibility that the reduction of vRNA and cRNA synthesis was caused by the reduction of viral protein synthesis, we carried out a viral model replicon assay (19, 30) in which active vRNP complexes were reconstituted with PB1, PB2, PA, and NP and the model vRNA encoding the luciferase gene, as described in Materials and Methods (Fig. 5F). With this system, we could examine the viral polymerase activity independent of the expression level of viral proteins since viral proteins were expressed from plasmids under the control of cellular RNA polymerase II promoter in this assay. Results shown in Fig. 5F indicate that vRNA, cRNA, and viral mRNA synthesis was decreased in RAF-2p48/UAP56 knockdown cells compared with that in control cells even in the presence of comparable amounts of NP in both cells. We found that NP synthesized in RAF-2p48/UAP56 knockdown cells migrates differently from that in control cells (Fig. 5F). Previous reports showed that NP is modified by phosphorylation (23) and that its N-terminal region is digested by caspase (35), but the involvement of RAF-2p48/UAP56 in these is not known at present.

It is well known that NP is one of proteins responsible for virus genome replication (15, 18, 27, 33). Recently, it is reported that ubiquitination of NP regulates virus genome replication (12). It is proposed that the soluble viral polymerase might act as a replicative enzyme in *trans*, but transcription occurs from template-bound viral polymerase in *cis* (8). In this study and recent reports (9, 31–33), *de novo* cRNA synthesis is found from template-bound viral polymerase; thus, it could be explained that the soluble viral polymerase might have stimulatory activity but is not completely essential for the synthesis of nascent cRNA. The viral nuclear export protein (NEP/NS2) is also involved in the accumulation level of vRNA and cRNA (26). Further, it is reported that small noncoding RNAs derived from the influenza virus genome might regulate viral transcription and replication through their interaction with viral polymerase complexes (21). To further understand the mechanism of influenza viral genome replication, precise analyses of a functional replicative enzyme including viral and cellular factors are required.

ACKNOWLEDGMENTS

We thank Y. Ishimi (Ibaraki University) for the generous gifts of baculoviruses expressing MCM proteins. This research was supported in part by a grant-in-aid from the Ministry of Education, Culture, Sports, Science, and Technology of Japan (to K.N. and F.M.) and Research Fellowships of the Japanese Society for the Promotion of Science (to A.K.).

REFERENCES

1. **Biswas, S. K., P. L. Boutz, and D. P. Nayak.** 1998. Influenza virus nucleoprotein interacts with influenza virus polymerase proteins. J. Virol. **72:**5493–5501.
2. **Blumberg, B. M., M. Leppert, and D. Kolakofsky.** 1981. Interaction of VSV leader RNA and nucleocapsid protein may control VSV genome replication. Cell **23:**837–845.
3. **Chan, W. H., et al.** 2010. Functional analysis of the influenza virus H5N1 nucleoprotein tail loop reveals amino acids that are crucial for oligomerization and ribonucleoprotein activities. J. Virol. **84:**7337–7345.
4. **Fleckner, J., M. Zhang, J. Valcarcel, and M. R. Green.** 1997. U2AF65 recruits a novel human DEAD box protein required for the U2 snRNP-branchpoint interaction. Genes Dev. **11:**1864–1872.
5. **Honda, A., et al.** 1990. Purification and molecular structure of RNA polymerase from influenza virus A/PR8. J. Biochem. **107:**624–628.
6. **Honda, A., K. Ueda, K. Nagata, and A. Ishihama.** 1988. RNA polymerase of influenza virus: role of NP in RNA chain elongation. J. Biochem. **104:**1021–1026.
7. **Horikami, S. M., J. Curran, D. Kolakofsky, and S. A. Moyer.** 1992. Complexes of Sendai virus NP-P and P-L proteins are required for defective interfering particle genome replication in vitro. J. Virol. **66:**4901–4908.
8. **Jorba, N., R. Coloma, and J. Ortin.** 2009. Genetic trans-complementation establishes a new model for influenza virus RNA transcription and replication. PLoS Pathog. **5:**e1000462.
9. **Kawaguchi, A., and K. Nagata.** 2007. De novo replication of the influenza virus RNA genome is regulated by DNA replicative helicase, MCM. EMBO J. **26:**4566–4575.
10. **Komissarova, N., J. Becker, S. Solter, M. Kireeva, and M. Kashlev.** 2002. Shortening of RNA:DNA hybrid in the elongation complex of RNA polymerase is a prerequisite for transcription termination. Mol. Cell **10:**1151–1162.
11. **Labadie, K., E. Dos Santos Afonso, M. A. Rameix-Welti, S. van der Werf, and N. Naffakh.** 2007. Host-range determinants on the PB2 protein of influenza A viruses control the interaction between the viral polymerase and nucleoprotein in human cells. Virology **362:**271–282.
12. **Liao, T. L., C. Y. Wu, W. C. Su, K. S. Jeng, and M. M. Lai.** 2010. Ubiquitination and deubiquitination of NP protein regulates influenza A virus RNA replication. EMBO J. **29:**3879–3890.
13. **Linder, P., and F. Stutz.** 2001. mRNA export: travelling with DEAD box proteins. Curr. Biol. **11:**R961–R963.
14. **Masters, P. S., and A. K. Banerjee.** 1988. Complex formation with vesicular stomatitis virus phosphoprotein NS prevents binding of nucleocapsid protein N to nonspecific RNA. J. Virol. **62:**2658–2664.
15. **Medcalf, L., E. Poole, D. Elton, and P. Digard.** 1999. Temperature-sensitive lesions in two influenza A viruses defective for replicative transcription disrupt RNA binding by the nucleoprotein. J. Virol. **73:**7349–7356.
16. **Momose, F., et al.** 2001. Cellular splicing factor RAF-2p48/NPI-5/BAT1/UAP56 interacts with the influenza virus nucleoprotein and enhances viral RNA synthesis. J. Virol. **75:**1899–1908.
17. **Nagata, K., A. Kawaguchi, and T. Naito.** 2008. Host factors for replication and transcription of the influenza virus genome. Rev. Med. Virol. **18:**247–260.
18. **Newcomb, L. L., et al.** 2009. Interaction of the influenza a virus nucleocapsid protein with the viral RNA polymerase potentiates unprimed viral RNA replication. J. Virol. **83:**29–36.
19. **Obayashi, E., et al.** 2008. The structural basis for an essential subunit interaction in influenza virus RNA polymerase. Nature **454:**1127–1131.
20. **Palese, P., P. Wang, T. Wolff, and R. E. O'Neill.** 1997. Host-viral protein-protein interactions in influenza virus replication, p. 327–340. *In* M. A. McCrae (ed.), Molecular aspects of host-pathogen interaction. Cambridge University Press, Cambridge, United Kingdom.
21. **Perez, J. T., et al.** 2010. Influenza A virus-generated small RNAs regulate the switch from transcription to replication. Proc. Natl. Acad. Sci. U. S. A. **107:**11525–11530.
22. **Poole, E., D. Elton, L. Medcalf, and P. Digard.** 2004. Functional domains of the influenza A virus PB2 protein: identification of NP- and PB1-binding sites. Virology **321:**120–133.
23. **Portela, A., and P. Digard.** 2002. The influenza virus nucleoprotein: a multifunctional RNA-binding protein pivotal to virus replication. J. Gen. Virol. **83:**723–734.

24. **Qanungo, K. R., D. Shaji, M. Mathur, and A. K. Banerjee.** 2004. Two RNA polymerase complexes from vesicular stomatitis virus-infected cells that carry out transcription and replication of genome RNA. Proc. Natl. Acad. Sci. U. S. A. **101:**5952–5957.
25. **Read, E. K., and P. Digard.** 2010. Individual influenza A virus mRNAs show differential dependence on cellular NXF1/TAP for their nuclear export. J. Gen. Virol. **91:**1290–1301.
26. **Robb, N. C., M. Smith, F. T. Vreede, and E. Fodor.** 2009. NS2/NEP protein regulates transcription and replication of the influenza virus RNA genome. J. Gen. Virol. **90:**1398–1407.
27. **Shapiro, G. I., and R. M. Krug.** 1988. Influenza virus RNA replication in vitro: synthesis of viral template RNAs and virion RNAs in the absence of an added primer. J. Virol. **62:**2285–2290.
28. **Shimizu, K., H. Handa, S. Nakada, and K. Nagata.** 1994. Regulation of influenza virus RNA polymerase activity by cellular and viral factors. Nucleic Acids Res. **22:**5047–5053.
29. **Strasser, K., et al.** 2002. TREX is a conserved complex coupling transcription with messenger RNA export. Nature **417:**304–308.
30. **Sugiyama, K., et al.** 2009. Structural insight into the essential PB1-PB2 subunit contact of the influenza virus RNA polymerase. EMBO J. **28:**1803–1811.
31. **Vreede, F. T., and G. G. Brownlee.** 2007. Influenza virion-derived viral ribonucleoproteins synthesize both mRNA and cRNA in vitro. J. Virol. **81:**2196–2204.
32. **Vreede, F. T., H. Gifford, and G. G. Brownlee.** 2008. Role of initiating nucleoside triphosphate concentrations in the regulation of influenza virus replication and transcription. J. Virol. **82:**6902–6910.
33. **Vreede, F. T., T. E. Jung, and G. G. Brownlee.** 2004. Model suggesting that replication of influenza virus is regulated by stabilization of replicative intermediates. J. Virol. **78:**9568–9572.
34. **Yamanaka, K., A. Ishihama, and K. Nagata.** 1990. Reconstitution of influenza virus RNA-nucleoprotein complexes structurally resembling native viral ribonucleoprotein cores. J. Biol. Chem. **265:**11151–11155.
35. **Zhirnov, O. P., T. E. Konakova, W. Garten, and H. Klenk.** 1999. Caspase-dependent N-terminal cleavage of influenza virus nucleocapsid protein in infected cells. J. Virol. **73:**10158–10163.

OPEN ACCESS Freely available online

PLoS one

Tamiflu-Resistant but HA-Mediated Cell-to-Cell Transmission through Apical Membranes of Cell-Associated Influenza Viruses

Kotaro Mori[☯], Takahiro Haruyama[☯¤], Kyosuke Nagata*

Department of Infection Biology, Faculty of Medicine and Graduate School of Comprehensive Human Sciences, University of Tsukuba, Tsukuba, Japan

Abstract

The infection of viruses to a neighboring cell is considered to be beneficial in terms of evasion from host anti-virus defense systems. There are two pathways for viral infection to "*right next door*": one is the virus transmission through cell-cell fusion by forming syncytium without production of progeny virions, and the other is mediated by virions without virus diffusion, generally designated cell-to-cell transmission. Influenza viruses are believed to be transmitted as *cell-free* virus from infected cells to uninfected cells. Here, we demonstrated that influenza virus can utilize cell-to-cell transmission pathway through apical membranes, by handover of virions on the surface of an infected cell to adjacent host cells. Live cell imaging techniques showed that a recombinant influenza virus, in which the *neuraminidase* gene was replaced with the *green fluorescence protein* gene, spreads from an infected cell to adjacent cells forming infected cell clusters. This type of virus spreading requires HA activation by protease treatment. The cell-to-cell transmission was also blocked by amantadine, which inhibits the acidification of endosomes required for uncoating of influenza virus particles in endosomes, indicating that functional hemagglutinin and endosome acidification by M2 ion channel were essential for the cell-to-cell influenza virus transmission. Furthermore, in the cell-to-cell transmission of influenza virus, progeny virions could remain associated with the surface of infected cell even after budding, for the progeny virions to be passed on to adjacent uninfected cells. The evidence that cell-to-cell transmission occurs in influenza virus lead to the caution that local infection proceeds even when treated with neuraminidase inhibitors.

Citation: Mori K, Haruyama T, Nagata K (2011) Tamiflu-Resistant but HA-Mediated Cell-to-Cell Transmission through Apical Membranes of Cell-Associated Influenza Viruses. PLoS ONE 6(11): e28178. doi:10.1371/journal.pone.0028178

Editor: Ron A. M. Fouchier, Erasmus Medical Center, The Netherlands

Received July 8, 2011; **Accepted** November 2, 2011; **Published** November 30, 2011

Funding: This work was supported in part by a grant-in-aid from the Ministry of Education, Culture, Sports, Science, and Technology of Japan (to KN: #20249025). The funders had no role in study design, data collection and analysis, decision to publish, or preparation of the manuscript. The authors received no additional external funding for this study.

Competing Interests: The authors have declared that no competing interests exist.

* E-mail: knagata@md.tsukuba.ac.jp

☯ These authors contributed equally to this work.

¤ Current address: Central Research Center, AVSS Corporation, Nagasaki, Japan

Introduction

It is generally accepted that viruses, released as *cell-free* virions from an infected cell, transmit to distant cells and tissues. This spreading pathway contributes to wide-ranged diffusion of *cell-free* viruses. However, in this spreading pathway, viruses are exposed to host anti-virus defense systems. In contrast, direct infection to a neighboring cell is considered to be beneficial for the virus in terms of evasion from the host anti-virus defense. There are two typical manners in infection to "*right next door*": one is the virus transmission through cell-cell fusion by forming syncytium without production of progeny virions, and the other is mediated by virions without virus diffusion, generally designated cell-to-cell transmission [1,2].

The cell-cell fusion infection pathway is characteristic for a variety of virus such as paramyxoviruses, herpesviruses, some retroviruses, and so on. For example in the case of measles virus belonging to *Paramyxoviridae*, infection is initiated by the interaction of the viral hemagglutinin glycoprotein with host cell surface receptors. The virus penetrates into the cell through membrane fusion mediated by the interaction of the fusion glycoprotein. In later stages of infection, newly synthesized glycoproteins accumulate at the cell membrane resulting in fusion of the infected cell with neighboring cells by producing syncytia. Thus, viruses can spread from cell to cell without producing *cell-free* virus particles.

The examples of the cell-to-cell transmission are diverse, and these mechanisms are dependent on pairs of viruses and host cells. Vaccinia virus particles bound on the filopodium of an infected cell are repelled toward neighboring uninfected cells by the formation of filopodia using actin filament [3]. The filopodia direct viruses to uninfected cells. Immunotropic viruses including retroviruses utilize an immunological synapse, designed as virological synapses for the cell-to-cell transmission [4–7]. Claudin-1 and occludin, components of tight junction, are involved in hepatitis C virus (HCV) entry through the cell-to-cell transmission [8,9]. The cell-to-cell transmission through tight junction is also observed in other viruses which infect epithelial layers [10,11]. These retroviruses and HCV remain on the surface of an infected cell even after budding. The uninfected cells adjacent to these infected cells can accept or take over viruses from

the infected cell. Thus, the cell-to-cell transmission can be categorized into two manners based on the state of infecting viruses, either *cell-free* or cell-associated virions.

Influenza virus, belonging to the family of *Orthomyxoviridae*, is one of the most serious zoonotic pathogens and causes seasonal epidemics or periodic pandemics among human beings around the world. The viral envelope consists of a lipid bilayer derived from cells that anchors three of viral transmembrane proteins, hemagglutinin (HA), neuraminidase (NA), and matrix protein 2 (M2). Influenza virus infection is initiated by the attachment of HA on virus particles to cell surface receptors containing sialic acids [12]. It has been known that the specific interaction between HA and sialic acid species is one of the determinants of the host range of influenza viruses [13]. Beside its role in the viral attachment, HA is also involved in intracellular fusion between viral envelope and host cell endosome membrane in the endocytotic pathway, by which the virus content is released inside the host cell [14]. The functional maturation of HA is mediated by the cleavage of HA into two disulfide-linked glycopolypeptides, HA1 and HA2 [15], accomplished by trypsin or trypsin-like proteases derived from host cells [16–19]. The membrane fusion is induced by a conformational change in the mature HA, which is triggered at low pH in the endosome, allowing viral ribonucleoprotein complexes to release into the cytoplasm [20,21]. Thus, HA plays a critical role in initiation and progression of influenza virus infection. Influenza virus NA possesses the enzymatic activity that cleaves α-ketosidic linkages between terminal sialic acids and adjacent sugar residues of cellular glycoconjugates [22]. The sialidase activity of NA removes terminal sialic acid residues from HA and NA proteins as well as host cell surface glycoproteins. Since the terminal sialic acid of sialyloligosaccharides is critical for HA binding, the receptor-destroying activity of NA serves to counter the receptor-binding activity of HA. It is quite likely that this activity contributes to prevention of successive superinfection of an infected cell [23]. In the absence of the functional sialidase activity, progeny virions aggregate on the cell surface due to the HA receptor-binding activity and can not be released [24,25]. Thus, NA cleaves sialic acids from the cell surface and facilitates virus release from infected cells. However, it is not clear whether every progeny virion is released as *cell-free* virion to infect the uninfected cells after diffusion into the extracellular environment. Influenza viruses are generally transmitted as *cell-free* viruses from infected to uninfected cell but they may also infect through the cell-to-cell transmission, in particular during local lesion formation.

Here, we examined whether influenza virus transmits from an infected cell to adjacent uninfected cells without virus release. Live cell imaging techniques showed that a recombinant influenza virus, in which the *NA* gene was replaced with the *green fluorescence protein* gene, spreads from an infected cell to adjacent cells forming infected cell clusters. Furthermore, progeny virions remain associated on the surface of infected cell even after budding, and then progeny virions could be passed to adjacent uninfected cells.

Results

Influenza virus can spread in an NA-independent manner to adjacent cells

To examine the transmission pathway of influenza virus, we performed immunofluorescence analyses by using anti-nucleoprotein (NP) polyclonal antibody. Influenza virus can form an infection center even in the presence of oseltamivir, a potent NA inhibitor (commercially known as Tamiflu) [26–28]. Oseltamivir at the concentration of 50 μg/ml completely prevented the release of progeny influenza viruses (Figure 1A). Noted that a large

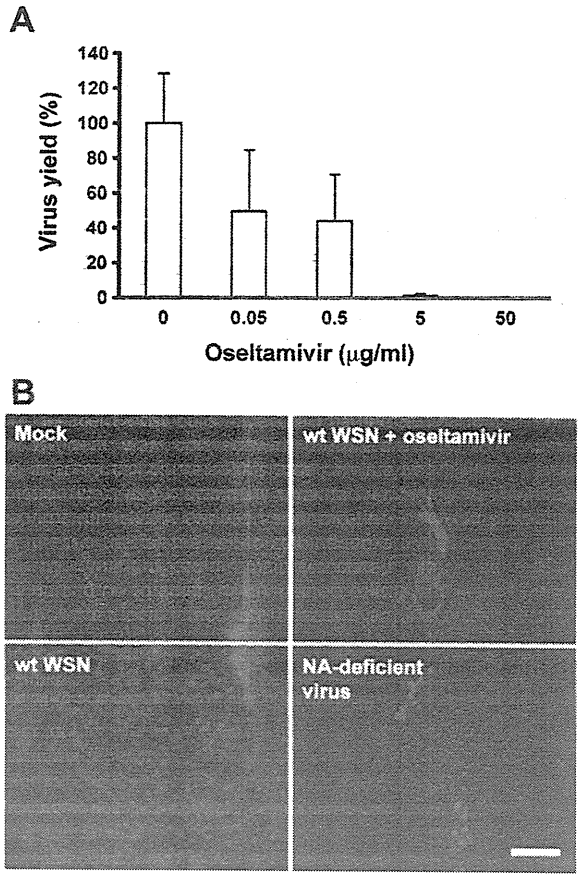

Figure 1. Influenza viruses can spread independent of the NA activity. (A) MDCK cells were infected with influenza virus A/WSN/33 at a multiplicity of infection (MOI) of 0.001 PFU per cell. At 48 hours post infection (hpi), culture supernatant was collected, and then its virus titer was determined by plaque assays. Each result was represented by a value relative to that in the absence of the drug. Error bars indicate standard deviation (s.d.) from 3 independent experiments. (B) Confluent MDCK cells were infected by wild-type influenza virus A/WSN/33 or NA-deficient influenza virus at MOI of 0.0001 in the presence or absence of 50 μg/ml oseltamivir phosphate. NA-deficient influenza virus was generated by reverse genetics as previously described [29]. After incubation at 37°C for 36 hours, immunofluorescence analyses were performed using anti-nucleoprotein (NP) polyclonal antibody and anti-rabbit IgG antibody conjugated to Alexa Fluor 568 (Invitrogen). Scale bar, 100 μm.
doi:10.1371/journal.pone.0028178.g001

number of single fluorescent foci caused by initial infection markedly expanded and formed cell clusters consisting of 5–10 infected cells in an MDCK cell monolayer (Figures 1B and S1), suggesting influenza virus can spread to some extent in the presence of oseltamivir. To verify that NA is not involved in this spreading, we generated an NA-deficient influenza virus by a reverse genetics method as described previously [29,30]. The NA-deficient influenza virus contains a mutated NA segment, in which the NA coding region including a sialidase catalytic domain was replaced with the *enhanced green fluorescent protein (EGFP)* gene [29]. By this replacement, the NA activity is eliminated from the recombinant influenza virus, and *EGFP* can be utilized as a marker for viral infections. Immunofluorescence analyses demonstrated that the NA-deficient influenza virus also forms infected cell

clusters similarly to those formed by wild-type influenza virus in the presence of oseltamivir (Figure 1B). The fluorescence pattern of NP overlapped with the localization of GFP derived from the *EGFP* gene of the NA-deficient influenza virus (Figure S2). Thus, NA-deficient influenza virus can be used to investigate the NA-independent infection pathway of influenza virus.

Next, we performed live cell imaging analyses to directly observe the infection time course of the NA-deficient influenza virus. The GFP fluorescence derived from the NA-deficient influenza virus first appeared in a single cell on an MDCK cell monolayer at 24 hours post infection. The virus started to spread from an infected cell to adjacent cells in 5–6 hours after the first appearance of a GFP-positive cell (Figure 2 and Video S1). The spreading rate was clearly faster than the rate of cell divisions. The mean doubling time of uninfected MDCK cells was 20–24 hours under the condition employed here, and it is expected that the proliferation speed would be much slowly because infected MDCK cells were maintained in the serum-free medium and formed cell monolayer at the high cell density. These suggest that NA-deficient influenza viruses may infect adjacent cells through the cell-to-cell transmission mechanism without apparent production of *cell-free* virions.

Cell-to-cell transmission pathway of influenza viruses is less sensitive to neutralizing antibody

The cell-to-cell virus transmission pathway could be interpreted as one of viral evolving strategies to avoid neutralizing antibody responses [2,31,32]. Therefore, we examined the effect of neutralizing antibody on NA-deficient influenza virus. A polyclonal antibody with the neutralizing activity against influenza virus particles inhibited infection of *cell-free* viruses to less than 50% at the concentration of 0.03%, although the cell cluster formation was observed at the concentration less than 0.01%. On the other hand, the NA-independent transmission of the NA-deficient influenza virus was blocked only when neutralizing antibody was present at the concentration of 0.3% (Figure 3). These results indicated that the NA-independent transmission of influenza viruses is less sensitive to the neutralizing antibody.

NA-independent transmission of influenza virus is HA-dependent

Next, to investigate the mechanism of NA-independent transmission of influenza virus, we examined whether HA is involved in this transmission. In the absence of the NA activity, virus spreading from an infected cell to adjacent cells was dramatically suppressed by omission of trypsin, essential for maturation of HA, from the experimental condition (Figure 4A). The GFP fluorescence derived from NA-deficient influenza virus appeared in a single cell at 24 hours post infection. However, this virus did not spread, but rather disappeared during subsequent 24 hours (Video S2). These observations indicate that the NA-independent cell-to-cell transmission of influenza virus is dependent on HA maturation mediated by trypsin, as is the case for the general *cell-free* transmission of this virus.

To clarify whether virus particles or viral RNP complexes are transmitted to adjacent cells, we examined the effect of amantadine on the cell-to-cell transmission of influenza virus. Amantadine inhibits the early step of uncoating of influenza virus RNP from virion in endosomes [33,34]. For this study, other influenza virus strain, influenza virus A/Udorn/72, was used instead of influenza virus A/WSN/33 because influenza virus A/WSN/33 is highly resistant to amantadine [35]. We confirmed that influenza virus A/Udorn/72 is sensitive to oseltamivir (Figure S3) and could also spread via cell-to-cell transmission independent of the NA activity as did for influenza virus A/WSN/33 (Figures 1B and 4B). In the case of a single administration of amantadine, fluorescent foci derived from infected cells scattered, and the number of single foci was greatly decreased compared

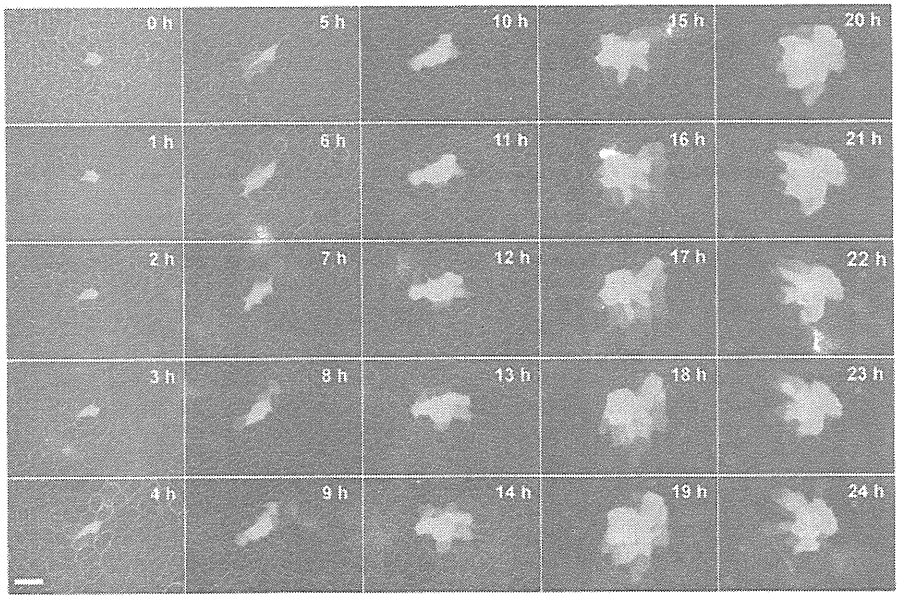

Figure 2. NA-deficient influenza virus spreads through cell-to-cell transmission. Confluent MDCK cells were infected with the NA-deficient influenza virus at MOI of 0.0001. After incubation at 37°C for 24 hours, a single GFP-positive cell, in which the recombinant virus replicated, was found at 1 hour after starting monitoring, and then this cell and its neighborhood were traced during the period from 24 hpi to 48 hpi at interval of 1 hour. Scale bar, 50 μm.
doi:10.1371/journal.pone.0028178.g002

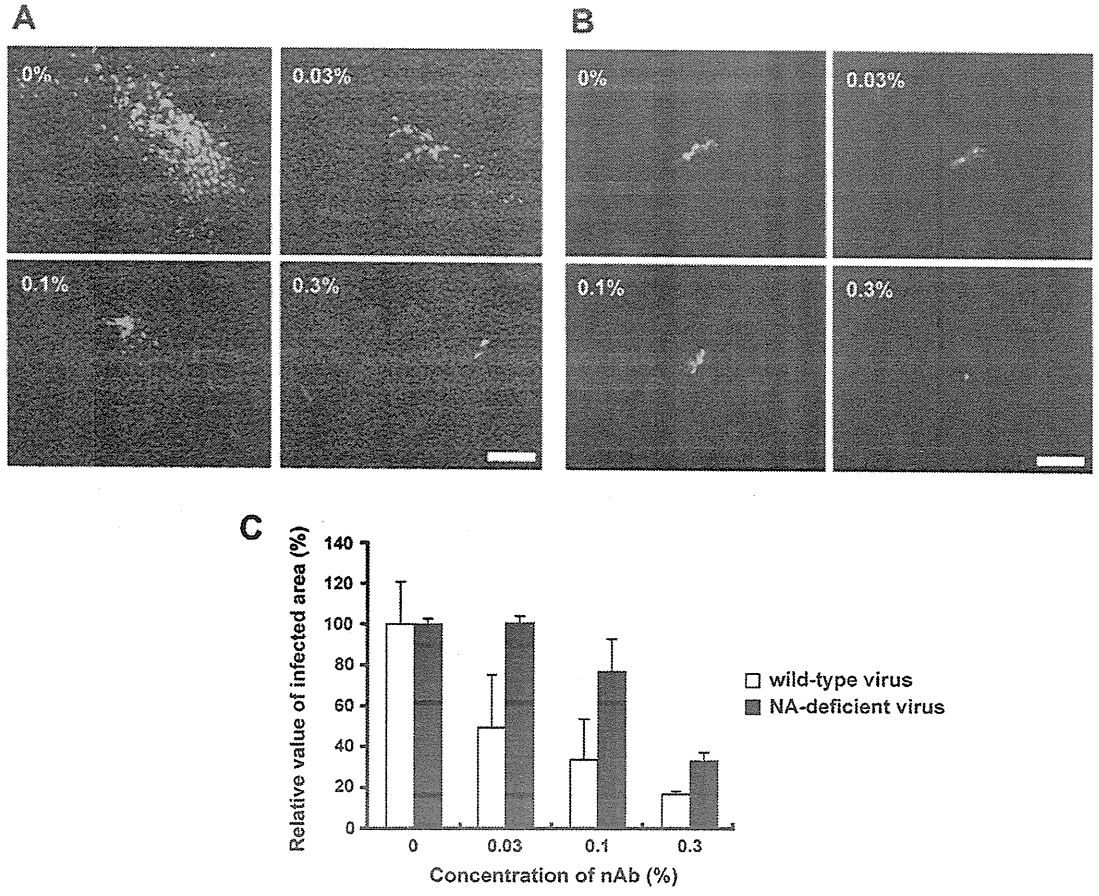

Figure 3. The cell-to-cell transmission of the NA-deficient influenza virus is less sensitive to the neutralizing antibody. (A) Infection of the wild-type and (B) NA-deficient influenza virus were performed in the presence or absence of antiserum containing neutralizing antibodies. Immunofluorescence analyses were performed with cells infected with wild-type influenza virus at 18 hpi using anti-NP antibody and anti-rabbit IgG antibody conjugated to Alexa Fluor 488 (Invitrogen). GFP fluorescence derived from the recombinant virus was observed at 36 hpi. Scale bar, 100 μm. (C) The level of viral spreading was indicated in the graph by measuring NP and GFP derived from wild-type and NA-deficient virus, respectively. Five different microscope fields were taken randomly, and then the intensity of green color was analyzed with ImageJ NIH image processing software. Each result was represented by a value relative to that in the absence of neutralizing antibodies. Error bars indicate s.d. from 3 independent experiments.
doi:10.1371/journal.pone.0028178.g003

with that in the absence of the drugs. In contrast, a single administration of oseltamivir, fluorescent foci formed some clusters and expanded in a time-dependent manner (Figure 4B). This dissimilarity of inhibitory manner was caused by the difference of the sites of action between amantadine and oseltamivir. Amantadine inhibits the replication of influenza A virus by preventing the translocation of vRNP complexes from endosomes to the cytoplasm, whereas oseltamivir has no effects on viral replication itself but inhibits the release of *cell-free* virions from infected host cells. We investigated the inhibitory effect of amantadine on the cell-to-cell transmission of influenza viruses. The formation of infected cell clusters was observed with co-administration of amantadine and oseltamivir, as well as with a single administration of oseltamivir (Figure 4B). However, the quantitative analysis revealed that the size of infected cell clusters with the co-administration were decreased as compared to that with oseltamivir alone (Figure 4C). These observations indicated that the NA activity-independent cell-to-cell transmission of influenza virus was susceptible to the inhibitory effect of amantadine, suggesting that the cell-to-cell transmission undergoes through endocytosis but vRNP complex itself is not incorporated in the infected cells by adjacent cells.

Cell-to-cell transmission occurs on the apical cell membrane

The virus transmission undergoes from infected to uninfected cells through either basolateral [36–38] or apical [39–42] sides. In the case of influenza virus, *cell-free* progeny virions are released only from the apical surface of polarized epithelial cells [43]. This releasing polarity is achieved by directed transport of viral membrane proteins to the apical plasma membrane [44]. Indeed, that HA and NA glycoproteins are associated with lipid rafts, and the raft association has been implicated in apical transport [45,46].

To determine whether or not the cell-to-cell transmission of the NA-deficient influenza virus occurs on the apical surface, we performed transwell assays in the presence of the neutralizing antibody to influenza A viruses. The neutralizing antibody was added to infected MDCK cell monolayer from apical or

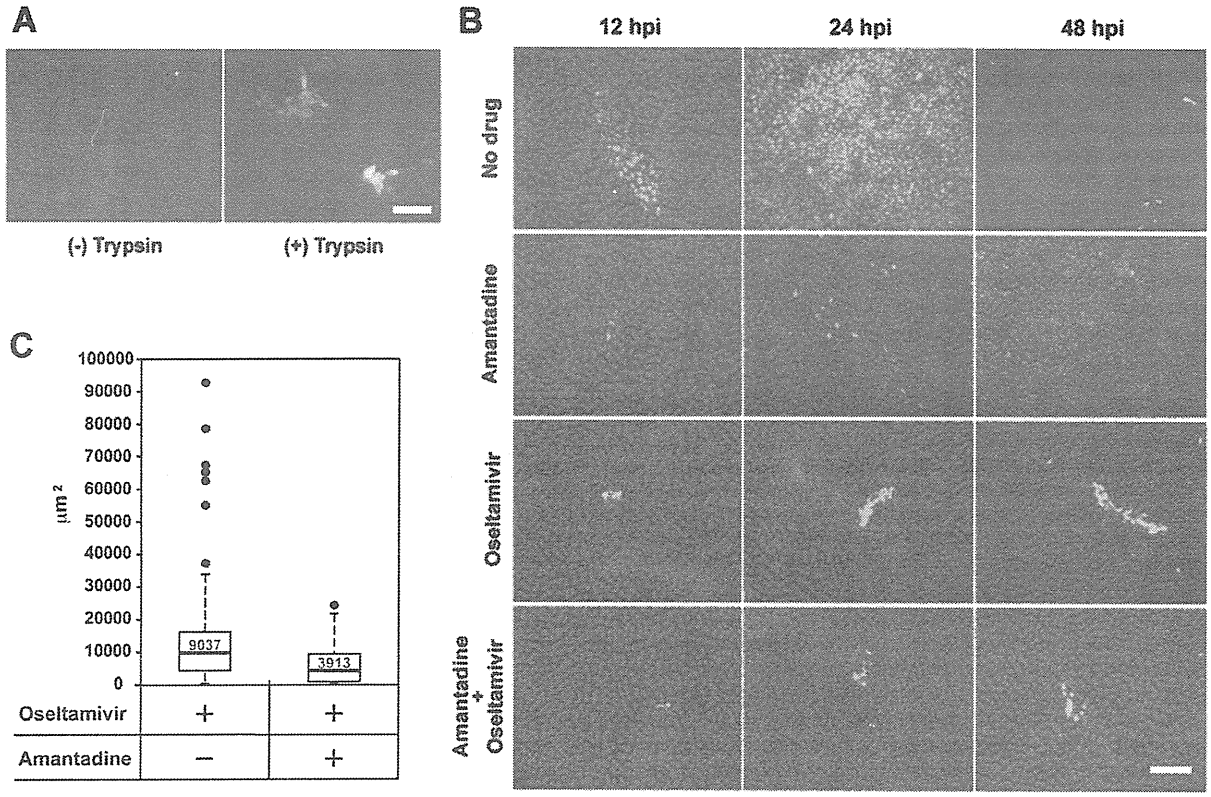

Figure 4. The cell-to-cell transmission of the NA-deficient influenza virus requires functional HA. (A) Confluent MDCK cells were infected with the NA-deficient influenza virus at MOI of 0.0001 in the presence or absence of 1 μg/ml trypsin. GFP fluorescence derived from the recombinant virus was observed at 36 hpi. Scale bar, 100 μm. (B) MDCK cells were infected with influenza virus A/Udorn/72 at moi of 0.0001 in the presence or absence of 50 μM amantadine or 50 μg/ml oseltamivir phosphate. Amantadine at the concentration of 50 μM almost completely inhibited the production of progeny virions (data not shown). After incubation for 12, 24, and 48 h, immunofluorescence analyses were performed using anti-NP antibody and anti-rabbit IgG antibody conjugated to Alexa Fluor 488 (Invitrogen). Viral NP and nuclear DAPI staining are shown in green and blue, respectively. Scale bar, 100 μm. (C) Median sizes of clusters were shown as box plots summarizing sizes of 60 individual infectious foci formed in the presence of oseltamivir alone, or both oseltamivir and amantadine. Immunofluorescence analyses were performed as described in (B) at 24 hpi. Boxes enclose the lower and upper quartiles; thick horizontal lines represent the median; dashed lines indicate the extreme values; and black dots are outliers of individual infectious foci. The size of infectious foci was measured with AxioVision Release 4.7.2 imaging software (Carl Zeiss). Median sizes shown in red letters were clearly different from each other ($p<0.01$).
doi:10.1371/journal.pone.0028178.g004

basolateral side, and the inhibitory effect on the spread of GFP fluorescence derived from the recombinant virus was examined. Addition of high concentrations of the neutralizing antibody from the apical side blocked the cell-to-cell transmission of the NA-deficient influenza virus, whereas the addition from the basolateral side had no effect (Figure 5). These observations indicated that the polarity in the influenza virus budding in the cell-to-cell transmission pathway is apical.

Influenza viruses can not re-infect previously infected cells

Previous report showed that influenza viruses were refractory to superinfection with a second cell-free virus [23]. In the case of the cell-to-cell transmission of influenza virus in the presence of oseltamivir, it is possible that a progeny virion is temporarily bridged by HA between an infected cell and adjacent uninfected cells, since viruses can not be released from infected cell surface due to the inhibition of the NA activity by oseltamivir. The cell-associated progeny virion may have an opportunity to re-infect the previously infected cell, compared to a cell-free progeny virion in the general spreading. Thus, we examined whether influenza viruses can infect the cell which had already been infected, using *ts*53 mutant and wild-type influenza virus A/WSN/33. *ts*53 virus has a substitution mutation from U to C at the nucleotide position of 701 in the PA gene. This substitution introduces an amino acid change from wild-type Leu 226 to Pro 226 and gives a defect in the viral genome replication process [47,48]. At first, cells were infected with *ts*53 virus at moi of 10, and after incubation for 0, 2, 4, 6, and 8 hours, cells were superinfected with wild-type virus at moi of 10. The amount of segment 3 viral RNA (vRNA) encoding PA was determined quantitatively by RT-PCR. Then, using a mutated primer for PCR, we could introduce a *Stu* I site only in the PCR products derived from the wild-type sequence (Figure 6A). Thus, DNA fragments amplified from the wild-type and *ts*53 could be distinguished by *Stu* I digestion. The digested DNA fragments containing 220 and 199 base pairs derived from *ts*53 and wild-type, respectively, were separated through PAGE. After 6 hours or later post infection, re-infection with the second challenging virus hardly occurs in the absence of oseltamivir. However, in the presence of oseltamivir, appearance of wild-type fragment suggests that the re-infection had occurred (Figure 6B). The result indicates